Reaction diffusion models in one dimension with disorder

Pierre Le Doussal

CNRS–Laboratoire de Physique Théorique de l'Ecole, Normale Supérieure, 24 rue Lhomond, F-75231 Paris, France

Cécile Monthus

Laboratoire de Physique Théorique et Modèles Statistiques, DPT-IPN, Bâtiment 100, 91400 Orsay, France
(Received 27 January 1999)

We study a large class of one-dimensional reaction diffusion models with quenched disorder using a real space renormalization group method (RSRG) which yields exact results at large time. Particles (e.g., of several species) undergo diffusion with random local bias (Sinai model) and may react upon meeting. We obtain a detailed description of the asymptotic states (i.e., attractive fixed points of the RSRG), such as the large time decay of the density of each specie, their associated universal amplitudes, and the spatial distribution of particles. We also derive the spectrum of nontrivial exponents which characterize the convergence towards the asymptotic states. For reactions which lead to several possible asymptotic states separated by unstable fixed points, we analyze the dynamical phase diagram and obtain the critical exponents characterizing the transitions. We also obtain a detailed characterization of the persistence properties for single particles as well as more complex patterns. We compute the decay exponents for the probability of no crossing of a given point by, respectively, the single particle trajectories (θ) or the thermally averaged packets ($\bar{\theta}$). The generalized persistence exponents associated to n crossings are also obtained. Specifying to the process $A+A \to \emptyset$ or A with probabilities $(r, 1-r)$, we compute exactly the exponents $\delta(r)$ and $\psi(r)$ characterizing the survival up to time t of a domain without any merging or with mergings, respectively, and the exponents $\delta_A(r)$ and $\psi_A(r)$ characterizing the survival up to time t of a particle A without any coalescence or with coalescences, respectively. $\bar{\theta}$, ψ, and δ obey hypergeometric equations and are numerically surprisingly close to pure system exponents (though associated to a completely different diffusion length). The effect of additional disorder in the reaction rates, as well as some open questions, are also discussed. [S1063-651X(99)15005-0]

PACS number(s): 05.70.−a

I. INTRODUCTION

A. Overview

Reaction diffusion processes are of wide interest in physics, chemistry, and biology [1]. In physics they present a relatively simpler case of nonequilibrium stochastic processes with nontrivial behavior. Traditionally they have been studied via mean-field-type methods (e.g., law of mass action, local chemical kinetics) [2]. However, in sufficiently low spatial dimension, particle density fluctuations become dominant and mean-field methods become invalid [3]. The role of fluctuations in these processes has thus been studied for a while, but has received renewed attention recently [4], as new exact results in one dimension [1] and systematic renormalization group studies have appeared [5]. One interest of these models is their relation to phase ordering kinetics via the ''coarsening'' of domain structures evolving towards equilibrium [6]. In some cases, these can be seen as reaction diffusion processes for defects, for instance domain walls in one dimension or XY-type vortices in two dimensions, which diffuse and can annihilate or coalesce upon meeting. These coarsening processes have also been much studied recently, especially in an effort to characterize their so-called persistence (or survival or first passage) properties for single spins, domains, or global magnetization [7–11].

Although many results are now available for reaction diffusion processes in homogeneous situations, comparatively little is known on their dynamics in the presence of quenched disorder, which is expected to play a role in many physical realizations. It can be introduced in the models in several ways, e.g., in the reaction rates or in the single particle diffusion. One can expect that it will strongly modify the behavior of the system in some cases by amplifying the role of spatial density fluctuations. These effects are interesting, but difficult to study analytically because of the present lack of methods, beyond mean-field approximations or perturbation theory, to treat the dynamics of such disordered systems.

Even in the absence of quenched disorder, there is an apparently unlimited variety of behaviors in reaction diffusion systems. The more complex ones, such as oscillatory or chaotic behaviors, become possible for a large enough number of species [12–15]. In simpler cases, attempts have been made to identify possible universality classes, and a wide class of models with finite reaction rates, amenable to field theoretical treatments, has been studied [16,17]. For instance, branching and annihilating random walks (BARW), i.e., reactions such as $A \to mA$ and $A+A \to 0$ or $A \to 0$, exhibit transitions from inactive (no particle) to active states, which were found to be either in the universality class of directed percolation [18–20] (odd number of offsprings) or in the so-called parity conserving class (even number of offsprings) [17]. This was confirmed by exact results in one dimension [21]. Related types of models describe epidemy propagation, such as $A+B \to 2B$ (with rate k), and either $B \to A$ (recovery) or $B \to C$ (immune) (rate $1/\tau$) were also studied via RG [22] (see [23] for review). The effect of quenched disorder has been studied in this class of BARW models, via random rates $k(x)$ and $\tau(x)$ but with limited success as the RG flows

to strong coupling [23]. As for directed percolation with disorder, it is still a largely open problem [24–26].

There is a simpler class of homogeneous models without branching (i.e., without particle production), such as $A+A \to 0$, $A+A \to A$ [27,28], $A+B \to 0$ [29,30], etc., which has still nontrivial behavior [31]. One interesting phenomenon is that in low enough dimension, the process becomes diffusion limited rather than reaction limited. Indeed particles in close proximity react quickly and the remaining particles are typically separated by a length related to the pure diffusion length $L_0(t) \sim (Dt)^{1/2}$. This leads to a decay of specie density, e.g., $n_A(t) \sim t^{-d/2}$ for $d<2$ in the case of $A+A \to 0$, slower than the mean-field prediction $n_A(t) \sim t^{-1}$ valid for $d>2$ (for $A+B \to 0$ a related argument leads $n_A(t) \sim t^{-d/4}$ for $d<4$) [29]. These types of results for such models in the pure case are well established from heuristic arguments, numerical simulations, perturbative RG [27,28,32], and in some cases rigorous methods [33,31]. It is now interesting to investigate how disorder will modify these behaviors. With disorder, models in this class are easier to study than the BARW-type models, although it is still a difficult task. The reactions $A+A \to 0$ and $A+B \to 0$ have been studied using perturbative field theoretic RG methods for particles diffusing in random flows, either in two dimensions [34,35] or in a special hydrodymamic flow [36]. As can be expected from the study of single particle diffusion in such flows [37,38], the behavior should be qualitatively different in the case of *potential* disorder, which tends to segregate the particles and slow the reaction (and the diffusion), than for *hydrodynamic* flows, which tend to mix the particles and increase the effective reaction rate (and lead to hyperdiffusion). The competition which arises when both components are present has been studied very recently in $d=2$ [34] and in $d=2-\epsilon$ [39]. Remarkably, the one-dimensional problem seems quite far from the reach of such perturbative RG methods and no generic result is available at present [40] in that case, hence the interest of the present study. Indeed, in $d=1$ only potential disorder can exist and is known to lead to ultraslow single particle diffusion described by a strong disorder (i.e., zero temperature) fixed point [41]. To make progress in $d=1$ requires developing nonperturbative techniques, which is the aim of the present work.

B. Model

In this paper we study a broad class of reaction diffusion models where particles diffuse on a one-dimensional lattice and can react or annihilate upon meeting. Apart from their reactions the particles are noninteracting. More specifically, each site of the lattice can be in one of several possible ''states,'' labeled $k=0,1,\ldots,n-1$. $k=0$ corresponds to the empty state with no particle present at that site. $k=1,\ldots,n-1$ corresponds to the presence of particles of different types. When two particles (i.e., states) $k_1>0$ and $k_2>0$ meet, they react and give another state k with a probability W_{k_1,k_2}^k. k may be the empty state $k=0$, corresponding to an annihilation. The reaction is thus a stochastic process

$$k_1+k_2 \to k \quad \text{with probability} \quad W_{k_1,k_2}^k \tag{1}$$

characterized by a fixed transition probability matrix which satisfies

$$\sum_k W_{k_1,k_2}^k = 1. \tag{2}$$

The matrix W_{k_1,k_2}^k can be extended to include $k_1=0$ by defining

$$W_{0,k'}^k = W_{k',0}^k = \delta_{k,k'} \tag{3}$$

for any k,k', which is the property expected for an empty state ($A+0 \to A$ with probability 1).

One prominent example will be identical particles A which react upon meeting as

$$
\begin{aligned}
A+A &\to \emptyset \quad \text{with probability } r, \\
A+A &\to A \quad \text{with probability } 1-r.
\end{aligned}
\tag{4}
$$
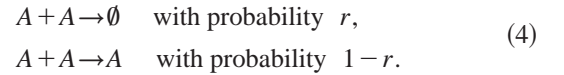
In this case there are only two states: $k=0$ corresponds to no particule present ($\emptyset$) and $k=1$ to one particule present A. The transition matrix is then $W_{0,0}^0 = W_{0,1}^0 = W_{1,0}^0 = W_{0,0}^1 = 0$, $W_{0,1}^1 = W_{1,0}^1 = 1$, and $W_{1,1}^0 = r, W_{1,1}^1 = 1-r$.

We will obtain results for processes within the above class (1) and study some specific examples. We will restrict ourselves to symmetric reaction rates $W_{k_1,k_2}^k = W_{k_2,k_1}^k$. Asymmetric rates, depending on the side from which the two species come in contact, can be defined in $d=1$ and can be studied by the same methods. We will mostly consider reaction diffusion processes with only a *finite* number of possible states (or species). Processes with an unbounded number of states ($n=\infty$) can also be studied by the present method, and we will give some examples. Classifying the much larger variety of complex behavior possible in that case is beyond the scope of the present study. Other extensions include randomness in the reaction rates, which we will briefly discuss in the end.

Up to now we have not specified the way in which particles diffuse, nor the reaction rates. Let us first concentrate on the process (4) and recall the known results in the case of pure diffusion (i.e., homogeneous hopping rates), which has been extensively studied. It is of particular interest in one dimension since it is also a model for zero temperature domain growth in the ferromagnetic q-states Potts model (with Glauber dynamics), where $r=1/(q-1)$ [11]. The case $q=2$ (Ising) corresponds to walkers (i.e., domain walls) always annihilating when they meet and $q=\infty$ to walkers always coagulating [42]. It is known that the reaction rate can be chosen infinite (immediate reaction upon meeting) without changing the universality class, and the same will hold here in the presence of disorder, hence our general choice of model (1). For all r the concentration of particles A is known to decrease as

$$n_A(t) \approx c(r)(Dt)^{-1/2}, \tag{5}$$

where the (*r-dependent*) coefficient is expected to be universal [e.g., $c(1)=(8\pi)^{-1/2}$ [43]]. More detailed properties, such as persistence, have also been studied. The probability $S(t)$ that no particle A (domain wall) has crossed a given point O up to time t has been shown to decay as

$$S(t) \sim L_0(t)^{-\theta(r)}, \qquad (6)$$

where $L_0(t) \sim \sqrt{t}$ is the characteristic length and $\theta(r)$ the so-called persistence exponent. $S(t)$ also corresponds to the probability that a spin has never been flipped up to time t in the Potts model. The exact expression of $\theta(r)$ was obtained in [11,44]. The domain size distribution has also been computed for this process in [45]. Two new independent exponents, ψ and δ, were introduced and studied in [46,47] to characterize the persistence (survival) of domains for this model, but as of now no exact result is available for these exponents. The concept of persistence properties was extended to other observables, finite temperature, and studied a variety of other models: persistence for global order parameter [10], spin block persistence [48], generalized persistence and large deviations [49,50], and persistence for fluctuating interfaces [51].

In this paper we study the case where the hopping rates are inhomogeneous with short range correlations, corresponding to random local bias. The generic model for this type of disorder is the Sinai model where each particle performs Arrhenius diffusion in the same energy landscape U_n where the local random forces $U_n - U_{n+1}$ are independent random variables of zero average (we restrict the present analysis to zero global bias). Various analytical results are known for the single particle Sinai model [52–58]. Diffusion is ultraslow as $x \sim L(t) = (\ln t)^2$. Recently we have reexamined this model [59,60] using a real space renormalization group method (RSRG) which yields exact results at long time. In the present paper we apply the RSRG method to study reaction diffusion of the type (1) for particles in a Sinai landscape. Some of the results have already appeared in [59]. Although we give here a detailed treatment of the reaction diffusion RSRG, we will rely on Ref. [60] for all details concerning the single particle diffusion aspects of the problem (which we will only sketch, referring the reader to [60] for details). Note that we consider here only models where all particles share the same diffusion property (i.e., see the same landscape and have the same diffusion coefficient). Thus this does not include reaction diffusion models such as Ising domain walls in a random field, for which a specific treatment is necessary and which are studied in [59,61]. Similarly, relations to other problems such as disordered quantum spin chains [62–65] or disordered free fermion models are discussed in [59,60]. In particular, we have chosen to discuss our present results exclusively in terms of reaction diffusion dynamics, and not in their equivalent formulation as (non-Hermitian) 1D quantum models (see [66] for details of such relations in the pure case). Finally, note that an exact RG has also been applied to the problem of coarsening of the pure 1D Φ^4 model at zero temperature for which persistence exponents have been computed [7,67].

As for the single particle problem, the RSRG method allows us to compute a number of quantities, and, remarkably, even some which are not known for the corresponding pure model (e.g., the domain persistence exponents δ and ψ). This makes the disordered case all the more interesting to study. We find that reaction diffusion processes in a Sinai landscape are strongly controlled by the ultraslow diffusion, e.g., the relevant length scale is the diffusion length $L(t) \sim (\ln t)^2$, but that they still possess nontrivial reaction prop-
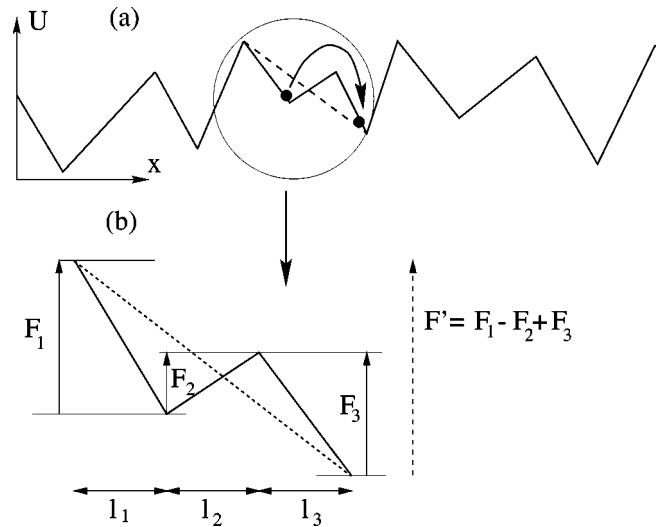

FIG. 1. (a) Energy landscape in the Sinai model (b) decimation method: the bond with the smallest barrier $F_{\min} = F_2$ is eliminated, resulting in three bonds being grouped into a single one.

erties. We will characterize a broad set of universality classes, containing all reactions of type (1). The reaction times (provided they are finite) do not affect any universal quantity, so that we can consider the reactions as instantaneous for practical purpose. As discussed in [60], there are other single particle diffusion models with short range correlated disorder in one dimension apart from Sinai's model universality class, such as random barriers (symmetric hopping rates) or random wells. For interesting behavior to occur, however, algebraically broad distributions are required from the start. Some results for reaction diffusion processes with this type of single particle diffusion have been obtained in [68].

The outline of the paper is as follows. In Sec. II we detail the RSRG method, first recalling known results in the case of a single particle in Sec. II A, then deriving the RSRG equation for reaction diffusion models in Sec. II B. The fixed points of this equation, and some physical properties of the corresponding asymptotic states, are studied in Secs. II C and II D, respectively. Section III is devoted to a detailed analysis of the dynamics near attractive or repulsive fixed points and of the convergence towards the asymptotic states. Throughout the paper we apply our results to the process (4) but in Sec. IV we discuss some applications to other examples of processes. In Sec. V we study persistence properties. Section VII contains the conclusion. Some more technical but useful details are contained in the Appendixes.

II. RSRG METHOD FOR REACTION DIFFUSION AND ASYMPTOTIC STATES

A. RSRG for Sinai landscape and single particle diffusion

The model for the diffusion of a single particle in one dimension can be defined, with no loss of generality [59], as the Arrhenius diffusion in a ''zigzag'' potential $U(x)$ represented in Fig. 1(a). It consists in a set of bonds, each bond (between x_i and x_{i+1}) being characterized by an energy barrier $F_i = |U_i - U_{i+1}|$ [where $U_i = U(x_i)$] and a length $l_i = |x_{i+1} - x_i|$. The energy landscape is chosen by choosing a

pair of bond variables F, l, independently from bond to bond, from a distribution $P(F, l)$ normalized to unity.

The RG procedure, which captures the long time behavior in a given energy landscape, is illustrated in Fig. 1(b) and consists in the iterative decimation of the bond with the *smallest barrier* [59], say F_2, and to replace the three bonds 1,2,3 by a single renormalized bond with barrier $F' = F_1 - F_2 + F_3$ and length $l' = l_1 + l_2 + l_3$. The new variables remain *independent* from bond to bond. To write the corresponding RG equation it is convenient to introduce Γ as the smallest remaining barrier at a given stage of the decimation and the rescaled variables $\eta = (F - \Gamma)/\Gamma$ and $\lambda = l/\Gamma^2$. The RG equation for the probability distribution [69] $P^\Gamma(\eta, \lambda)$ reads [59]

$$[\Gamma \partial_\Gamma - (1 + \eta)\partial_\eta - 2\lambda\partial_\lambda - 3]P^\Gamma(\eta, \lambda)$$
$$= P^\Gamma(0, \cdot) *_\lambda P^\Gamma(\cdot, \cdot) *_{\eta, \lambda} P^\Gamma(\cdot, \cdot) \qquad (7)$$

and coincides with the one derived in [63] for the closely related problem of disordered quantum spin chains. The symbol $*_\lambda$ denotes a convolution with respect to λ only and $*_{\eta, \lambda}$ with respect to both η and λ. The probability distribution is normalized to unity as $\int_0^{+\infty} d\eta \int_0^{+\infty} d\lambda P^\Gamma(\eta, \lambda) = 1$.

The landscape is characterized by the large scale variance of the potential

$$\overline{(U_i - U_j)^2} \approx 2\sigma|l_{i-j}| \qquad (8)$$

with l_{i-j} the distance from site i to site j, which is exactly preserved by the RG. Thus we will set $\sigma = 1$ in the following. Restoring σ simply amounts to a rescaling of lengths, and in particular σ drops out of all (universal) ratios of lengths that we consider later. As shown in [63,64], the RG equation (7) leads at large Γ (using Laplace transforms) to the following fixed point $P^*(\eta, \lambda)$:

$$P^*(\eta, \lambda) = LT_{s \to \lambda}^{-1}\left(\frac{\sqrt{s}}{\sinh\sqrt{s}} e^{-\eta\sqrt{s}\coth\sqrt{s}}\right). \qquad (9)$$

Thus for large Γ one finds that the average bond length $\bar{l}_\Gamma$ and the number of bonds n_Γ per unit length are [70], respectively,

$$\bar{l}_\Gamma = \frac{1}{2}\Gamma^2, \qquad n_\Gamma = \frac{2}{\Gamma^2}. \qquad (10)$$

The renormalized landscape allows us to study the dynamics of a single walker starting from a given point O at $t = 0$. The decimation of barriers smaller than

$$\Gamma = T\ln t \qquad (11)$$

corresponds to the elimination of (logarithmic) time scales shorter than the Arrhenius time t for the particle to cross the barrier. We are choosing everywhere time units such that the (nonuniversal) microscopic attempt time scale t_0 be set to unity [arbitrary units can be recovered by setting $\Gamma = T\ln(t/t_0)$ in what follows [71]]. Since at long time (i.e., large Γ) the renormalized landscape consists entirely of deep valleys separated by high barriers, a good approximation to the long time dynamics is to place the walker *at the bottom*

of the renormalized valley at scale $\Gamma = T\ln t$ which contains the starting point O, since with high probability it will be near to that point [52]. Upon proper rescaling of space and time this approximation becomes in fact *exact* as Γ tends to $+\infty$. This defines what we will call the "effective dynamics" in the following and is illustrated in Fig. 1. This allows us to recover the scaling $x \sim (\ln t)^2$ for the single particle diffusion as well as many other exact results detailed in [59,60]. Since it is customary, when studying reaction diffusion processes, to compare densities of reactants with a characteristic scale of diffusion, we give here the the exact expression for the single particle root-mean-square displacement, or "diffusion length" at large time:

$$\sqrt{\langle x^2(t)\rangle} \approx \frac{1}{6}\sqrt{\frac{61}{5}}T^2(\ln t)^2. \qquad (12)$$

To study reaction diffusion processes it will be necessary to consider "valleys" (two consecutive bonds sharing a common potential minimum). We thus slightly generalize the above RG equation (7) to follow the distribution of renormalized valleys. The RG equation for the valley probability distribution $P^\Gamma(\eta_1, \eta_2)$ at scale Γ in rescaled variables (η_1, η_2) reads

$$\Gamma\partial_\Gamma P^\Gamma(\eta_1, \eta_2)$$
$$= [(1 + \eta_1)\partial_{\eta_1} + (1 + \eta_2)\partial_{\eta_2} + 2]P^\Gamma(\eta_1, \eta_2)$$
$$+ P^\Gamma(\eta_1, \cdot) *_{\eta_2} P^\Gamma(0, \cdot) + P^\Gamma(\cdot, 0) *_{\eta_1} P^\Gamma(\cdot, \eta_2), \qquad (13)$$

where we have omitted (i.e., integrated over) the lengths for simplicity. The large time (Γ) behavior of this equation can be studied similarly. Valley distributions which have the decoupled form $P^\Gamma(\eta_1, \eta_2) = P^\Gamma(\eta_1)P^\Gamma(\eta_2)$, where $P^\Gamma(\eta)$ satisfies the bond RG equation (7), are of course solution of the RG equation for valleys (13). The subspace of such decoupled distributions (called decoupled subspace in the following) is thus preserved by RG. Since the initial condition is uncorrelated, the RG flow defined by Eq. (13) remains in this decoupled subspace, and converges towards the fixed point $P^*(\eta_1, \eta_2) = P^*(\eta_1)P^*(\eta_2) = e^{-\eta_1 - \eta_2}$. This convergence result extends to the case of small correlations between valley sides as will be discussed below.

It was shown in [64] that the convergence towards the bond fixed point $P^*(\eta) = e^{-\eta}$ is like $1/\Gamma$ with eigenvector $(1 - \eta)e^{-\eta}$. Thus the convergence towards the valley fixed point $P^*(\eta_1, \eta_2) = e^{-\eta_1 - \eta_2}$ within the decoupled subspace is of the form

$$\left(e^{-\eta_1} + \frac{c}{\Gamma}(1 - \eta_1)e^{-\eta_1} + \cdots\right)$$

$$\times\left(e^{-\eta_2} + \frac{c}{\Gamma}(1 - \eta_2)e^{-\eta_2} + \cdots\right)$$

$$= e^{-\eta_1 - \eta_2}\left(1 + \frac{c}{\Gamma}(2 - \eta_1 - \eta_2)\right) + \cdots \qquad (14)$$

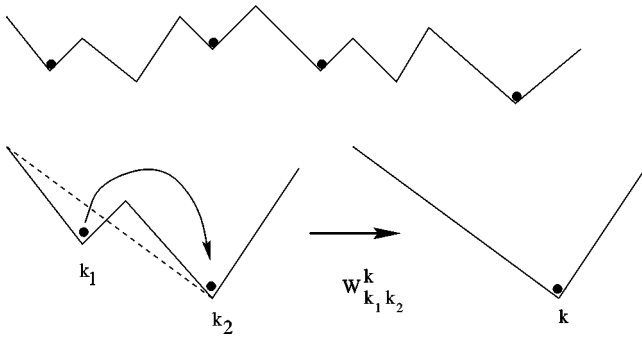and is also as $1/\Gamma$ with eigenvector $(2 - \eta_1 - \eta_2)e^{-\eta_1 - \eta_2}$.

FIG. 2. (a) Macroscopic state of the reaction diffusion process: each renormalized valley is either empty ($k=0$) or contains a particle of type $k>0$ (b) at time scale t such that the barrier $F=\Gamma = T\ln t$ is decimated, the state (particle) k_1 in the decimated valley moves to the neighboring valley and reacts with k_2 to produce k with probability W_{k_1,k_2}^k, as the two valleys are merged into a single renormalized one containing k.

B. RG equations for reaction diffusion

We now turn to diffusion reaction models of type (1) in one-dimensional landscapes with random local biases.

From the results on the dynamics of a single particle in a Sinai landscape recalled in the preceding section, it is clear that one can study most of the properties of the initial reaction diffusion problem by following its evolution under the effective dynamics. It also becomes obvious that one must now consider valleys, and the species contained in these valleys. At the decimation time scale $\Gamma = T\ln t$ in some places in the system, two valleys will merge into one and the reaction (1) governed by the rates matrix W will take place. This process is illustrated in Fig. 2. The errors made by this approximation are expected to become again smaller at large time, as will be discussed later on.

The general method to study the process (1) is thus to associate to each valley the specie which it contains, which is one of several possible states k ($k=0$ being the empty state). A convenient initial model is thus one where each valley and its content is statistically independent and characterized by a probability distribution $P_k^\Gamma(\eta_1,\eta_2)$ with $\Sigma_k P_k^\Gamma(\eta_1,\eta_2)=P^\Gamma(\eta_1,\eta_2)$. It remains so under the RG. The effective dynamics is described by the RG equation:

$$\Gamma \partial_\Gamma P_k^\Gamma(\eta_1,\eta_2)$$
$$= [(1+\eta_1)\partial_{\eta_1}+(1+\eta_2)\partial_{\eta_2}+2]P_k^\Gamma(\eta_1,\eta_2)$$
$$+ W_{k_1,k_2}^k [P_{k_1}^\Gamma(\eta_1,\cdot)*_{\eta_2}P_{k_2}^\Gamma(0,\cdot)$$
$$+ P_{k_1}^\Gamma(\cdot,0)*_{\eta_1}P_{k_2}^\Gamma(\cdot,\eta_2)], \qquad (15)$$

where summation over repeated indices is implied. The summation over k yields back the valley RG equation (13). Since the average length of a valley is $2\bar{l}_\Gamma$, the total concentration $n_k(t)$ of a given specie k (the total number of k particles per unit of length) is given as

$$n_k(t)=\frac{1}{2}n_\Gamma p_k^\Gamma, \qquad (16)$$

where

$$p_k^\Gamma = \int_{\eta_1,\eta_2} P_k^\Gamma(\eta_1,\eta_2) \qquad (17)$$

and n_Γ is the number of remaining bonds (10) per unit length at scale $\Gamma=T\ln t$. We stress that the RG equation (15) is more complicated to analyze than Eq. (13) since it cannot in general be factorized into bond distributions.

However, it turns out that there is still a simple subspace of distributions which is exactly preserved by the RG equation (15). It is the subspace of functions of the sum $\eta_1 + \eta_2$,

$$P_k^\Gamma(\eta_1,\eta_2)=H_k^\Gamma(\eta=\eta_1+\eta_2), \qquad (18)$$

where the functions $H_k(\eta)$ satisfies

$$\Gamma \partial_\Gamma H_k^\Gamma(\eta)=[(2+\eta)\partial_\eta+2]H_k^\Gamma(\eta)$$
$$+ W_{k_1,k_2}^k H_{k_1}^\Gamma(\cdot)*_\eta H_{k_2}^\Gamma(\cdot), \qquad (19)$$

which conserves the normalization $\Sigma_k p_k^\Gamma = \int_0^\infty d\eta\ \eta\Sigma_k H_k^\Gamma(\eta)$. This subspace plays an important role in the following. Already one sees that both the fixed point $e^{-\eta_1-\eta_2}$ and the leading eigenvector $(2-\eta_1-\eta_2)e^{-\eta_1-\eta_2}$ of the linearized landscape RG equation (13) belong to this subspace.

C. Fixed points of the RG equations and asymptotic states

We now determine the fixed point solutions of the RG equation for the valley distributions (15). We already know that the sum $\Sigma_k P_k^\Gamma(\eta_1,\eta_2)=P^\Gamma(\eta_1,\eta_2)$ converges towards the fixed point of Eq. (13) $P^*(\eta_1,\eta_2)=e^{-(\eta_1+\eta_2)}$ which describes the landscape. It is thus natural to look for fixed points of Eq. (15) of the following form:

$$P_k^*(\eta_1,\eta_2)=p_k^* \ P^*(\eta_1,\eta_2)=p_k^*e^{-(\eta_1+\eta_2)}, \qquad (20)$$

where $p_k^*\geq 0$ and $\Sigma_k p_k^*=1$ by normalization. Plugging this form into Eq. (15) leads to a consistent Γ-independent solution if the p_k^* satisfy the condition

$$p_k^* = W_{k_1,k_2}^k p_{k_1}^* p_{k_2}^*. \qquad (21)$$

Note that any solution of this equation satisfies *a priori* $\Sigma_k p_k^*=0$ or 1, as a consequence of Eq. (2). Thus apart from the unphysical solution of Eq. (21) where all p_k^* vanish, all other solutions are automatically correctly normalized.

In general, Eq. (21) has several solutions and thus there are several fixed points to the valley equations (15). Clearly some of these fixed points are attractive and correspond to possible large time asymptotic states for the reaction diffusion process while other fixed points are repulsive. In some cases several attractive fixed points can coexist and lead to a nontrivial phase diagram.

The stability of each fixed point, as well as their convergence property, will be studied in detail in the next section. Here we just mention one important result. The dynamics in the vicinity of a fixed point p_k^* is determined by the following stability matrix:

$$M_{kj} = W^k_{k',j} p^*_{k'}. \tag{22}$$

We denote by μ_α the eigenvalues of M, and by p^α_j the associated eigenvectors $M_{kj} p^\alpha_j = \mu_\alpha p^\alpha_k$. For $n-1$ reacting species (in addition to the empty state $k=0$), M is an n-dimensional matrix with non-negative elements. One eigenvalue is trivial, being simply $\mu_1=1$ of eigenvector $p^{\alpha=1}_k \propto p^*_k$ (21). The other $n-1$ eigenvalues μ_α ($\alpha = 2, \ldots, n$), which can be complex in general, have a smaller modulus, due to the Perron-Froebenius theorem. We will focus in the following on simple enough processes where all μ_α are real, but we will also give example of more general reaction diffusion where complex eigenvalues arise (e.g., reactions with cycles).

Let us consider here only fixed points with all μ_α being real. The result of the next section is that, in that case, a given fixed point if attractive is the $n-1$ eigenvalues $\mu_\alpha < 1/2$ for $\alpha = 2, \ldots, n$. It is repulsive if at least one of these $\mu_\alpha > 1/2$ (and is then repulsive along the corresponding eigendirection).

For example, in the case of the reaction diffusion process (4), there are two solutions of Eq. (21) and thus two fixed points. One is the empty state $E = (p^*_0 = 1, p^*_A = 0)$ and the other is $S = (p^*_0 = r/(1+r), p^*_A = 1/(1+r))$. The stability matrix associated to E is simply the 2×2 identity matrix (i.e., $\mu_1 = 1 = \mu_2$) and this fixed point is thus repulsive. The matrix associated to the state S reads $M_S = ((r/r+1, r/r +1), (1/(r+1), 1/(r+1)))$ with eigenvalues $\mu_1 = 1$ and $\mu_2 = 0$. The fixed point S is thus attractive and corresponds to the asymptotic state which represents the large time behavior of the system.

In fact, the reaction diffusion process (4) possesses an interesting property: the outcome of a sequence of reactions does not depend on the order it was performed. We call these processes ''associative processes.'' They have the property that $M^2 = M$, i.e., $\mu = 0, 1$. Some properties of these associative processes are detailed in Appendix B.

D. Physical properties of the asymptotic states

We now study some physical consequences. Each attractive fixed point corresponds to a possible large time behavior of the system, i.e., an asymptotic state. If there are several attractive fixed points, the one chosen by the system will depend on the initial value of the parameters (mainly the specie concentrations).

From the results (20) and (10) we obtain that in an asymptotic state [characterized by a set of p^*_k solution of Eq. (21)], the density of specie k behaves at large time as

$$n_k(t) = \frac{1}{2} n_\Gamma p^*_k = \frac{p^*_k}{T^2 \ln^2(t/t_0)}, \tag{23}$$

where we have restored the microscopic attempt time scale t_0 [72]. Note that this result (23) represents the leading large time contribution; subleading corrections (which become dominant only if $p^*_k = 0$) will be determined in the next section. Interestingly, this leading behavior is independent of the initial concentration (provided it is in the basin of attraction of the fixed point). This universality property can be

further characterized by computing universal amplitudes. In pure models a commonly studied amplitude is the product of specie concentration by the diffusion volume. In a disordered model one has more choices of definitions, but we will define an amplitude as in [39]. Here we find the exact result for the following *universal amplitude* (associated to specie k):

$$\mathcal{A}_k \equiv \lim_{t \to \infty} n_k(t) \sqrt{\overline{\langle x^2(t) \rangle}} = p^*_k \frac{1}{6} \sqrt{\frac{61}{5}}. \tag{24}$$

This gives, for instance, $\mathcal{A}(r) = 1/(1+r) \frac{1}{6} \sqrt{\frac{61}{5}}$ for the process (4), i.e., $\mathcal{A} = 0.291\,071 \ldots$ for $A + A \to 0$ studied in [39] by perturbative methods [73].

From the statistical independence of valleys in an asymptotic state, information about the spatial distribution of the species can also be obtained. For instance, one can define ''domains'' in the simplest case as intervals between particles (i.e., between nonempty states $k \neq 0$, irrespective of their content). We can now compute exactly the distribution of the size of ''domains.'' From the above form of the fixed points, the normalized distribution $D_\Gamma(l)$ of domain sizes l in an asymptotic state takes a scaling form $D_\Gamma(l) = (1/\Gamma^2) D^*(\lambda = l/\Gamma^2)$ which can be computed as follows.

The above RG equation for valley distributions (15) can be readily extended to $P_k(\eta_1, \eta_2, \lambda_1, \lambda_2)$ which takes into account the rescaled lengths $\lambda_1 = l_1/\Gamma^2$, $\lambda_2 = l_2/\Gamma^2$ of the two bonds of the valley, extending Eq. (7). The generalized fixed point (20) reads

$$P^*_k(\eta_1, \eta_2, \lambda_1, \lambda_2) = p^*_k P^*(\eta_1, \lambda_1) P^*(\eta_2, \lambda_2), \tag{25}$$

where $P^*(\eta, \lambda)$ is the fixed point solution (9) of the bond RG equation. A domain as defined above is thus a set of consecutive empty valleys between two occupied valleys, together with one bond in each of the occupied valleys (see Fig. 2). Since in the asymptotic state valleys are statistically independent and are either empty ($k=0$) with probability $p^*_0 P^*(\lambda_1) P^*(\lambda_2)$ [where $P^*(\lambda) = \int_\eta P^*(\lambda)$] or contain a particle ($k \neq 0$) with probability $(1 - p^*_0) P^*(\lambda_1) P^*(\lambda_2)$, one easily obtains the Laplace transform of $D^*(\lambda)$ as

$$\hat{D}^*_{p^*_0}(s) = \int_0^{+\infty} d\lambda \ e^{-s\lambda} D^*(\lambda)$$

$$= \frac{(1 - p^*_0) P^*(s)^2}{1 - p^*_0 P^*(s)^2} = \frac{1 - p^*_0}{\cosh^2 \sqrt{s} - p^*_0}, \tag{26}$$

where we have used the explicit form (9) for the fixed point bond distribution. Formula (26) can be inverted and yields the distribution of rescaled domain sizes:

$$D^*_{p^*_0}(\lambda) = \tan\alpha \sum_{n=-\infty}^{+\infty} (\alpha + n\pi) e^{-\lambda(\alpha + n\pi)^2}, \tag{27}$$

$$= \frac{\tan\alpha}{\sqrt{\pi}\lambda^{3/2}} \sum_{m=-\infty}^{+\infty} m \sin(2\alpha m) e^{-m^2/\lambda} \tag{28}$$

with $\alpha = \arccos p^*_0$.

This can be applied, e.g., in the case of the process (4). Substituting $p_0^* = r/(1+r)$ in Eq. (28) yields the distribution of distances between neighboring walkers A. Note that the case where walkers A always coalesce upon meeting ($r = 0, p_0 = 0$) corresponds to $\alpha \to \pi/2$ and in this limit Eq. (28) becomes

$$D_{p_0^*=0}^*(\lambda) = \sum_{n=-\infty}^{+\infty} [2\lambda \pi^2 (n+1/2)^2 - 1] e^{-\lambda \pi^2 (1/2+n)^2} \tag{29}$$

$$= \frac{2}{\sqrt{\pi} \lambda^{3/2}} \sum_{m=-\infty}^{+\infty} (-1)^{m+1} m^2 e^{-m^2/\lambda}. \tag{30}$$

It is interesting to compare the result (28) concerning the disordered case with the result of Derrida and Zeitak [45] for the case of homogeneous hopping rates. For small domain sizes ($\lambda \to 0$), the distribution vanishes much faster in the disordered case [as $\sim \lambda^{-3/2} \exp(-1/\lambda)$] than in the pure case (as $\sim \lambda$). For large domain sizes ($\lambda \to \infty$), both have exponentially decaying behavior (except for $q = +\infty$, i.e., $r = 0$ in the pure case). In addition, in the present case the consecutive domains lengths are statistically independent, which is not the case for the pure system.

The above calculation is easily generalized to compute the distribution of relative distances between two walkers of a given species k, simply by substituting $p_0^* \to 1 - p_k^*$ in the above formula (28).

III. DYNAMICS NEAR FIXED POINTS AND ASYMPTOTIC STATES

In this section we study the dynamics near the possible fixed points of the valley RG equation (attractive and repulsive).

We will first focus strictly on the effective dynamics exactly described by the RG equation (15), and mention some possible corrections in the real dynamics at the end of the section.

For the effective dynamics we will solve the problem in two steps. As mentioned above, the matrix M in Eq. (22) and its eigenvalues μ_α control the asymptotic dynamics. Interestingly they readily provide an approximation of the dynamics, which we will call the ''uniform approximation,'' which is interesting as it allows us to classify the spectrum of eigenperturbations and, in the case of real eigenvalues, already allows us to see whether a given fixed point is stable or unstable.

In a second step we will obtain the exact results for the spectrum of eigenperturbations.

A. First step: Uniform approximation

It is natural to define the total occupation probability of specie k at scale $\Gamma = T \ln t$ as $p_k^\Gamma = \int_{\eta_1, \eta_2} P_k^\Gamma(\eta_1, \eta_2)$. The difficulty of the problem comes from the fact that it does not satisfy a closed equation. However, if one also introduces $p_k^\Gamma(0) = \int_{\eta_2} P_k^\Gamma(0, \eta_2) = \int_{\eta_1} P_k^\Gamma(\eta_1, 0)$, i.e., the occupation

probability of specie k of the valleys just being decimated at Γ, one can obtain a closed coupled equation by integration of Eq. (15), which reads

$$\Gamma \partial_\Gamma p_k^\Gamma = 2[-p_k^\Gamma(0) + W_{k_1,k_2}^k p_{k_1}^\Gamma(0) p_{k_2}^\Gamma]. \tag{31}$$

It is then tempting to set, as an approximation, $p_k^\Gamma(0) = p_k^\Gamma$. This would be correct at any of the fixed points (20), but since we are studying convergence to a fixed point, it is an approximation which amounts to neglecting the dynamical correlations between the deviations in the specie concentration and in the distribution of barriers heights. For this reason we call it the ''uniform approximation.'' It yields the following approximate closed RG equation for the p_k^Γ:

$$\Gamma \partial_\Gamma p_k^\Gamma = 2(-p_k^\Gamma + W_{k_1,k_2}^k p_{k_1}^\Gamma p_{k_2}^\Gamma), \tag{32}$$

which preserves the normalization condition $\Sigma p_k = 1$. This approximate flow has the same fixed points $p_k^\Gamma = p_k^*$ as the true one (21). This equation, remarkably, is reminiscent of a ''mean-field type'' rate equation, except that the role of ''time'' would be played by the variable $\ln(T \ln t)$.

The relaxation of Eq. (32) towards any of these fixed points is studied by setting $p_k^\Gamma = p_k^* + f_k^\Gamma$ and linearizing for the small perturbation f_k^Γ around the fixed point p_k^*. It yields, in terms of the matrix M introduced in Eq. (22),

$$\Gamma \partial_\Gamma f_k^\Gamma = 2(-f_k^\Gamma + 2 M_{kk'} f_{k'}^\Gamma), \tag{33}$$

and thus the convergence towards the fixed point has components behaving as $\Gamma^{-\Lambda_\alpha}$, where the exponents are given in terms of the eigenvalues μ_α of the matrix M as $\Lambda_\alpha = 2(1 - 2\mu_\alpha)$ with $\alpha = 2, \ldots, n$.

So this ''uniform approximation'' would indicate that a fixed point is stable if all $\text{Re}(\mu_\alpha) < 1/2$ for all $\alpha = 2, \ldots, n$, and unstable otherwise. Remarkably, this stability criterion coincides with the exact result *when the eigenvalues are real* as we will now show, even if the naive convergence eigenvalues Λ_α are not correct (they are ''renormalized'' to larger absolute values).

B. Second step: Full dynamics near a fixed point

Up to now we have studied the convergence of the landscape alone (13), and the convergence of the p^Γ within a uniform approximation assuming $p^\Gamma(0) = p^\Gamma$.

We now study the full dynamics near a fixed point solution of the full reaction diffusion equations (15). We will indeed find that there are some correlations between deviations in total occupation probabilities (from the fixed point concentrations) and deviations in the barrier distribution profile (from the simple fixed point shape $e^{-\eta}$), resulting in deviations with respect to the uniform approximation.

We thus consider a perturbation around the fixed point of the form

$$P_k^\Gamma(\eta_1, \eta_2) = [p_k^* + c_k^\Gamma(\eta_1, \eta_2)] e^{-(\eta_1+\eta_2)} \tag{34}$$

and linearize the equation for the perturbation $c_k^\Gamma(\eta_1, \eta_2)$,

$$\Gamma \partial_\Gamma c_k^\Gamma(\eta_1, \eta_2)$$

$$= [(1+\eta_1)\partial_{\eta_1} - \eta_1 + (1+\eta_2)\partial_{\eta_2} - \eta_2] c_k^\Gamma(\eta_1, \eta_2) \tag{35}$$

$$+ M_{k_1,k_2}\left(\int_0^{\eta_1} d\eta' [c_{k_1}^\Gamma(\eta', \eta_2) + c_{k_1}^\Gamma(\eta', 0)]\right.$$

$$\left. + \int_0^{\eta_2} d\eta' [c_{k_1}^\Gamma(\eta_1, \eta') + c_{k_1}^\Gamma(0, \eta')]\right), \tag{36}$$

where we have used the symmetry of the W, and the definition of the matrix M (22).

Note that in the end we are interested in the behavior of the species proportions

$$p_k^\Gamma = \int_{\eta_1, \eta_2} P_k^\Gamma(\eta_1, \eta_2) = p_k^* + \epsilon_k^\Gamma,$$

where

$$\epsilon_k^\Gamma = \int_{\eta_1, \eta_2} c_k^\Gamma(\eta_1, \eta_2) e^{-(\eta_1 + \eta_2)}. \tag{37}$$

The normalization condition of course implies that $\Sigma_k \epsilon_k^\Gamma = 0$.

Decomposing $c_k^\Gamma(\eta_1, \eta_2)$ upon the eigenvectors p_k^α corresponding to the eigenvalues μ_α of the matrix M as $c_k^\Gamma(\eta_1, \eta_2) = \Sigma_\alpha c_\alpha^\Gamma(\eta_1, \eta_2) p_k^\alpha$, we obtain decoupled equations for the coefficients $c_\alpha^\Gamma(\eta_1, \eta_2)$,

$$\Gamma \partial_\Gamma c_\alpha^\Gamma(\eta_1, \eta_2)$$

$$= [(1+\eta_1)\partial_{\eta_1} - \eta_1 + (1+\eta_2)\partial_{\eta_2} - \eta_2] c_\alpha^\Gamma(\eta_1, \eta_2) \tag{38}$$

$$\mu_\alpha \left(\int_0^{\eta_1} d\eta' [c_\alpha^\Gamma(\eta', \eta_2) + c_\alpha^\Gamma(\eta', 0)]\right.$$

$$\left. + \int_0^{\eta_2} d\eta' [c_\alpha^\Gamma(\eta_1, \eta') + c_\alpha^\Gamma(0, \eta')]\right). \tag{39}$$

For a given μ_α, we look for solutions behaving as $c_\alpha^\Gamma \sim \Gamma^{-\Phi_\alpha}$ and determine the exponent Φ_α as a function of the eigenvalue μ_α. Here, *a priori* both μ_α and Φ_α can be complex.

Before we study this equation for general μ we will first study the simpler cases $\mu=0$ and $\mu=1$. Note that for associative processes this will be sufficient.

1. Study for $\mu_\alpha = 0$

This case is important for naively stable fixed points of associative processes (which have all $\mu_\alpha = 0$ for $\alpha = 2, \ldots, N-1$). The Γ-dependent equation (38) with $\mu_\alpha = 0$ can be integrated out explicitly starting from its initial value at Γ_0,

$$c_\alpha^\Gamma(\eta_1, \eta_2) = \left(\frac{\Gamma}{\Gamma_0}\right)^2 e^{-[(\Gamma/\Gamma_0)-1](\eta_1+\eta_2+2)}$$

$$\times c_\alpha^{\Gamma_0}\left(\frac{\Gamma}{\Gamma_0}(1+\eta_1)-1, \frac{\Gamma}{\Gamma_0}(1+\eta_2)-1\right), \tag{40}$$

and thus the convergence of proportions p_k^Γ towards p_k^* is governed by Eq. (37),

$$\epsilon_\alpha^\Gamma = \int_0^\infty d\eta_1 \int_0^\infty d\eta_2 c_\alpha^\Gamma(\eta_1, \eta_2) e^{-(\eta_1+\eta_2)}$$

$$= \int_{(\Gamma/\Gamma_0)-1}^\infty dy_1 \int_{(\Gamma/\Gamma_0)-1}^\infty dy_2 c_\alpha^{\Gamma_0}(y_1, y_2) e^{-(y_1+y_2)}. \tag{41}$$

So for generic initial perturbations $c_\alpha^{\Gamma_0}(\eta_1, \eta_2)$ that are not exponentially growing as $\eta_{1,2} \to \infty$, we obtain that the convergence towards the fixed point is exponential in Γ. Note that here this exact result is very different from the naive approximation which would predict a convergence as $\Gamma^{-\Lambda}$ with $\Lambda = 2$. To understand why this is so, one can compute from the exact solution (41) the ratio

$$\frac{p_k^\Gamma(0) - p_k^*}{p_k^\Gamma - p_k^*} \sim \frac{\Gamma}{\Gamma_0}, \tag{42}$$

which is found to grow with Γ. This is why the uniform approximation is particularly bad for this case where it predicts a power law instead of the exponential convergence in Γ.

2. Study for $\mu_\alpha = 1$

To study the dynamics (38) in the case $\mu_\alpha = 1$, it is useful to introduce the function $h_\alpha^\Gamma(\eta_1, \eta_2) = \partial_{\eta_1}\partial_{\eta_2} c_\alpha^\Gamma(\eta_1, \eta_2)$, since it satisfies the closed simpler equation

$$\Gamma \partial_\Gamma h_\alpha^\Gamma(\eta_1, \eta_2) = [(1+\eta_1)\partial_{\eta_1} + (1+\eta_2)\partial_{\eta_2}$$

$$+ 2 - \eta_1 - \eta_2] h_\alpha^\Gamma(\eta_1, \eta_2) \tag{43}$$

that gives after integration from an initial condition at Γ_0

$$h_\alpha^\Gamma(\eta_1, \eta_2) = \left(\frac{\Gamma}{\Gamma_0}\right)^4 e^{-[(\Gamma/\Gamma_0)-1](\eta_1+\eta_2+2)}$$

$$\times h_\alpha^{\Gamma_0}\left(\frac{\Gamma}{\Gamma_0}(1+\eta_1)-1, \frac{\Gamma}{\Gamma_0}(1+\eta_2)-1\right), \tag{44}$$

and thus for initial conditions $h_\alpha^{\Gamma_0}(\eta_1, \eta_2)$ that are not exponentially growing at $\eta_{1,2} \to \infty$, we obtain that the function h_α^Γ converges towards 0 exponentially in Γ. This means that the perturbations c_α^Γ converge exponentially in Γ towards the decoupled subspace

$$c_\alpha^\Gamma(\eta_1, \eta_2) = \psi_\alpha^\Gamma(\eta_1) + \psi_\alpha^\Gamma(\eta_2). \tag{45}$$

We now study the convergence towards the fixed point in that decoupled subspace to see if there are solutions behaving as $\psi_\alpha^\Gamma(\eta) \sim \Gamma^{-\Phi_\alpha}\psi_\alpha(\eta)$: the equation for $\psi_\alpha(\eta)$ reads

$$-\Phi_\alpha \psi_\alpha(\eta) = [(1+\eta)\partial_\eta - \eta]\psi_\alpha(\eta)$$

$$+ 2\int_0^\eta d\eta' \psi_\alpha(\eta') + \eta\psi_\alpha(0). \tag{46}$$

The only well-behaved solutions are found to be

$$\Phi_\alpha = +1, \quad \psi(\eta) = \psi_\alpha(0)(1-\eta), \quad (47)$$

$$\Phi_\alpha = -2, \quad \psi(\eta) = \psi_\alpha(0)(1+2\eta). \quad (48)$$

The first solution corresponds to the convergence as $1/\Gamma$ of the landscape discussed previously. This is not surprising since the linearized RG equation (13) is exactly Eq. (38) with $\mu = 1$. Note that Eq. (44) shows that small correlations between barriers in the same valley decrease exponentially fast in Γ towards the subspace of statistically independent distributions. Since this landscape eigenvector satisfies $\epsilon_\alpha^\Gamma = \int_{\eta_1,\eta_2} c_\alpha^\Gamma(\eta_1,\eta_2) e^{-(\eta_1+\eta_2)} = 0$, it does not affect the species proportions p_k^Γ. It is the second eigenvector in Eq. (48) which is relevant for the reaction diffusion processes since $\epsilon_\alpha^\Gamma \neq 0$. It corresponds to the unstable eigenvalue (growth as Γ^2) associated to a naively unstable fixed point (e.g., of an associative process). Note that in that case, the unstable eigenvalue found $\Phi = -2$ coincides with the naive value $\Lambda = 2(1-2\mu) = -2$ of the uniform approximation.

Physically, this eigenvalue can be understood for, e.g., the process (4). The unstable fixed point is the empty state E with $p_0 = 1$, $p_A = 0$. Now if one starts at t' very close to the fixed point, there are very few A and their number should not vary at first, as they will rarely meet. This is indeed exactly what the above result says, namely,

$$n_A(t) = \frac{1}{2} n_\Gamma p_A^\Gamma \sim \frac{1}{T^2 \ln^2 t}\left(p_A^* + [p_A(t') - p_A^*]\frac{\ln^2 t}{\ln^2 t'} \right) \quad (49)$$

and using that E has $p_A^* = 0$.

3. Study for general μ

We now study the case of a general μ_α. It turns out that one can find the solution of the original Eq. (38) under the form

$$c_\alpha^\Gamma(\eta_1,\eta_2) = \Gamma^{-\Phi_\alpha} H_\alpha(\eta_1+\eta_2), \quad (50)$$

where the function $H_\alpha(z)$ satisfies the differential equation

$$0 = (2+z)H_\alpha''(z) + (\Phi_\alpha+1-z)H_\alpha'(z) + (2\mu_\alpha-1)H_\alpha(z) \quad (51)$$

together with the boundary condition $2H_\alpha'(0) + \Phi_\alpha H_\alpha(0) = 0$.

The only well-behaved solution at $z \to \infty$ is the confluent hypergeometric function $H_\alpha(z) = U(1-2\mu_\alpha, 3+\Phi_\alpha, 2+z)$, and the boundary condition at $z = 0$ determines the possible exponents Φ_α that should satisfy $2U'(1-2\mu_\alpha, 3+\Phi_\alpha, 2) + \Phi U(1-2\mu_\alpha, 3+\Phi_\alpha, 2) = 0$. Using the identity $zU'(A,B,z) - (z+1-B)U(A,B,z) = -U(A-1,B-1,z)$, this equation for Φ_α reduces to
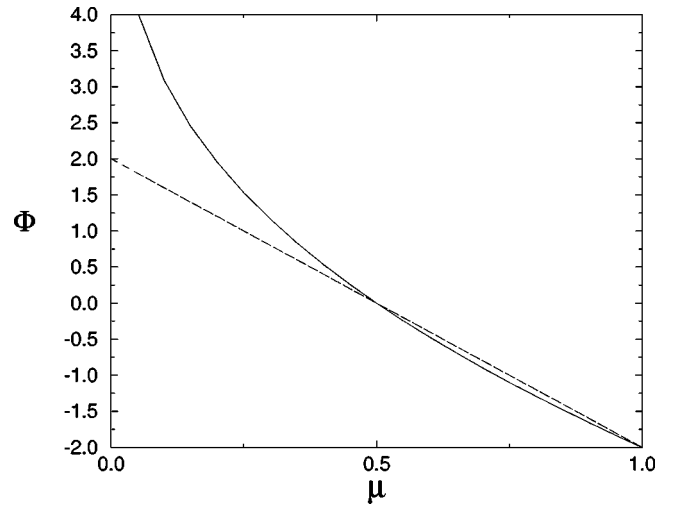
$$U(-2\mu_\alpha, 2+\Phi_\alpha, 2) = 0. \quad (52)$$

FIG. 3. Plot of the exponent Φ (Φ^-) as a function of the eigenvalue μ. It vanishes at $\mu = 1/2$ and diverges as $\mu \to 0$. The result of the uniform approximation is plotted as a dashed line.

We now discuss the behavior of the solutions of this equation. One must distinguish two cases.

4. Real μ

Let us start with μ real. As mentioned above, one must have $\mu \leq 1$. For $\mu = 1$, Eq. (52) reduces to $\Phi^2 + \Phi - 2 = 0$, which admits the two roots $\Phi = 1$ and $\Phi = -2$ and one thus recovers the eigenvalues (48). Equation (52) continues to admit two finite roots when μ belongs to the interval $\frac{1}{2} < \mu \leq 1$, which we denote $\Phi^+(\mu)$ and $\Phi^-(\mu)$ [with $\Phi^+(1) = 1$ and $\Phi^-(1) = -2$]. The behavior of these roots as a function of μ is plotted in Figs. 3 and 4. As μ is decreased from 1, $\Phi^+(1)$ increases and diverges when $\mu \to 1/2^+$ while $\Phi^-(\mu)$ increases from -2 to $\Phi^-(1/2) = 0$. For $\mu < 1/2$, Eq. (52) admits only one finite root $\Phi(\mu) = \Phi^-(\mu)$ which is positive and with $\Phi(1/2) = 0$ and $\Phi(\mu) \to +\infty$ as $\mu \to 0^+$.

Again we can see from the exact solution above why the uniform approximation is not valid. In terms of the dominant α mode, the ratio
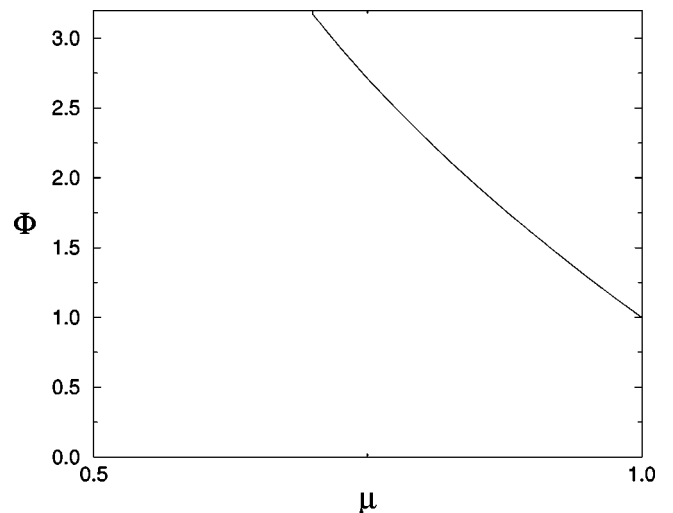

FIG. 4. Plot of the exponent Φ^+ as a function of the eigenvalue μ. It diverges at $\mu = 1/2$.

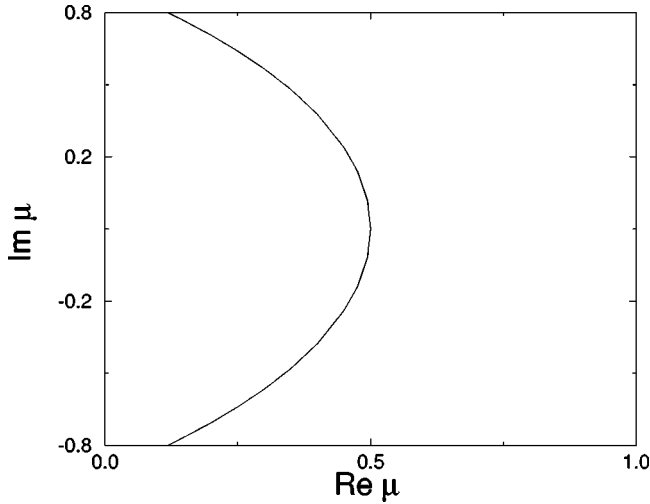FIG. 5. Stability diagram: the solid line in the complex plane of μ delimits the region of instability [$\text{Re}(\Phi)<0$ to the right of the line] from the region of stability [$\text{Re}(\Phi)>0$ to the left].

$$\frac{p_k^\Gamma(0)-p_k^*}{p_k^\Gamma-p_k^*}\sim\frac{\int_0^\infty dz H_\alpha(z)e^{-z}}{\int_0^\infty dz z H_\alpha(z)e^{-z}}\equiv b_\alpha \qquad (53)$$

goes at large Γ towards the finite limit b_α found to be bigger than 1 when $\mu<1/2$. One can check that setting $p_k^\Gamma=p_k^*+f_k^\Gamma$ and $p_k^\Gamma(0)=p_k^*+bf_k^\Gamma$ in Eq. (31), one obtains that the relaxation towards the fixed point is now like $\Gamma^{-\lambda_\alpha(b)}$ with $\lambda_\alpha(b)=2[b-(b+1)\mu_\alpha]$. Since $b_\alpha>1$, the correct exponent $\Phi_\alpha=\lambda_\alpha(b_\alpha)$ is bigger than the naive exponent $\Lambda_\alpha=\lambda_\alpha(b=1)$.

5. Complex μ

Next we turn to complex μ. The matrix M being real, if it has complex eigenvalues they will come in pairs, μ_α and μ_α^* corresponding to complex conjugate eigenvectors p_k^α and $(p_k^\alpha)^*$. In the uniform approximation they will combine as $f_k^\Gamma=\Gamma^{-\text{Re}(\Lambda_\alpha)}r_k\cos[\text{Im}(\Lambda_\alpha)\ln\Gamma+\phi_k^\alpha]$ and correspond to oscillatory (growing or decaying) solutions [where $\Lambda=2(1-2\mu)$ is complex]. This situation happens in cyclic reactions, examples of which will be given below. Within the uniform approximation the fixed point is stable to this perturbation if $\text{Re}(\mu)<1/2$ and unstable otherwise. This, however, turns out *not* to be correct. Indeed the correct exponent Φ (now complex) is determined by the above Eq. (52) associated to μ. One has $\Phi(\mu^*)=\Phi(\mu)^*$, and to each pair of μ, μ^* one can associate one (or two in some cases) pair of Φ,Φ^* also corresponding to oscillatory solutions. The oscillation frequency in the $\ln\Gamma$ variable is now given by $\text{Im}(\Phi)$, and the stability being now determined by $\text{Re}(\Phi)$ [$\text{Re}(\Phi)>0$ corresponds to a stable eigenperturbation, while $\text{Re}(\Phi)<0$ corresponds to an unstable one].

Interestingly, $\text{Re}(\Phi(\mu))$ is a decreasing function of $\text{Im}(\mu)>0$ as it is increased from 0. Thus the region of stability in the complex μ plane is *different* from the one inferred from the uniform approximation. It is represented in Eq. (5). One notes that for complex eigenvalues one can

have a fixed point naively stable [with $\text{Re}(\mu)<1/2$] which is in reality unstable [with $\text{Re}(\Phi)<0$].

C. Asymptotic dynamics: Conclusion

Thus we have solved the problem of the dynamics near the asymptotic states of the form (21) for arbitrary reaction diffusion process. Let us summarize the results.

When the eigenvalues μ_α of the matrix M (22) are real, the stability of the fixed point is determined by the following naive argument: a fixed point is stable if $\mu_\alpha<1/2$ for all $\alpha=2,\ldots$. The decay exponents Φ_α are obtained in terms of the μ_α as

$$\Phi_\alpha=F[\mu_\alpha], \qquad (54)$$

where the function $F[x]$ is defined implicitly by the single root of the equation $U[-2x,2+F[x],2]=0$ (here $0<x<1/2$) and represented in Fig. 3.

In terms of these exponents, the large time behavior for the concentrations of the species is found to be

$$n_k(t)=\frac{1}{2}n_\Gamma p_k^\Gamma, \qquad (55)$$

$$p_k=p_k^*+\sum_{\alpha=2,n}\frac{b_k^\alpha}{(T\ln t)^{\Phi_\alpha}}+\cdots, \qquad (56)$$

$$n_\Gamma=\frac{2}{T^2(\ln t)^2}\left(1+\frac{c}{T(\ln t)}+\cdots\right), \qquad (57)$$

where the $O(1/\Gamma)$ correction in n_Γ comes from the convergence of the landscape [74]. In addition, there are corrections to Eq. (55) which decay must faster, exponentially in Γ (i.e., algebraically in time). The b_k^α are constants, depending on the initial condition. The formula (55) can also be used to relate two late times. If the system is very near the asymptotic state at t', with $p_k(t')=p_k^*+\epsilon_k$, Eq. (55) holds at t with $b_k^\alpha=\epsilon_\alpha p_k^\alpha(T\ln t')^{-\Phi_\alpha}$, where we recall that the p_k^α are the eigenvectors of M and $\epsilon_k=\Sigma_\alpha\epsilon_\alpha p_k^\alpha$.

For practical applications it is useful to note that ratios of concentrations of different species involve only the exponents Φ_α. On the other hand, because of the factor n_Γ, the relaxation of the concentration of a single specie k to its asymptotic form is controlled (provided $p_k^*>0$) by the exponent $\min(1,\Phi)$ [where Φ is the minimum of all exponents Φ_α appearing in the corresponding formula (55) for $n_k(t)$]. The formula is even more interesting in the case $p_k^*=0$ (i.e., if the specie k disappears in the reaction) since then the first correction becomes the dominant decay and one has at large time that $n_k(t)\sim 1/(T\ln t)^{2+\Phi}$. Examples of such cases are studied in Sec. V D.

Let us stress again that the difference between the exact value Φ_α and the uniform approximation value Λ_α is due to the fact that near the asymptotic states the ratios $p_k^\Gamma(0)/p_k^\Gamma$ differ from 1, i.e., the valleys to be decimated do not have the average distribution of species: there is a nontrivial mixing between valley heights and concentration of species, missed by the naive argument, and responsible for the nontrivial relaxation exponents found here.

When some eigenvalues μ_α of the matrix M (22) are complex, the fixed point is stable provided all μ_α lie in the part of the complex plane on the left of the curve represented in Fig. 5. The specie concentrations then relax with oscillations as

$$n_k(t) = \frac{1}{2} n_\Gamma \left(p_k^* + \sum_{\alpha=2,n} \frac{b_k^\alpha}{(T \ln t)^{\text{Re}(\Phi_\alpha)}} \right.$$

$$\left. \times \cos[\text{Im}(\Phi_\alpha)\ln(T \ln t) + \phi_k^\alpha] + \cdots \right). \quad (58)$$

Finally, in the case where $\mu = 1/2$ [or more generally on the line $\text{Re}(\Phi) = 0$], linear analysis is insufficient to determine the evolution of the system, and one must study the full nonlinear RG equation (15), which goes beyond the present study [75].

To conclude this section, let us recall that the results derived above concern, strictly speaking, the effective dynamics described by the RG equation (15). As was discussed in great details in Ref. [60] for the single particule diffusion, there are corrections in the real dynamics, with respect to the effective dynamics. Indeed, in the effective dynamics the whole thermal packet jumps at $T \ln t = \Gamma$ over a barrier Γ, while in the real dynamics typically a fraction of a thermal packet [which can be written as $1 - \exp(-e^{-\Gamma[1-(T \ln t)/\Gamma]/T})$] has not yet jumped at time t. Since the distribution of barriers becomes broader and broader, this generates corrections which at large time are only subdominant for most quantities [at most $O(1/\Gamma)$] coming typically from rare events such as degeneracy of order $O(T)$ between neighboring barriers. They become dominant only for certain quantities, such as the width of the thermal packet, which have vanishing leading order in the effective dynamics. In Ref. [60] the corrections to first order in $O(1/\Gamma)$ were evaluated and found to originate from three rare events: (a) valleys with degenerate minima, (b) almost degenerate barriers, and (c) valleys just being decimated with a barrier $\Gamma + \epsilon$ (see Fig. 7 of [60]).

A similar detailed study of the rare events in the presence of reaction processes can be performed but goes beyond the present paper. With similar arguments as in [60], we do not expect any correction to the leading order of the quantities computed in this paper. In principle, subdominant corrections could add to the subleading terms computed above, e.g., in Eq. (55). They are certainly at most of order $O(1/\Gamma)$ (and thus cannot affect any decay as $\Gamma^{-\Phi}$ with $\Phi < 1$) but it is likely that they are even of higher order. Indeed most of these corrections [e.g., (b)] come from single particle diffusion and can be reabsorbed into the global factor n_Γ. Other events [such as (a)] cannot affect specie concentrations. Although this point deserves further study, it is likely that the corrections from the real dynamics to the convergence to asymptotic states obtained in this section are subdominant.

IV. EXAMPLES OF PROCESSES

Up to now we have only applied the general results to the process (4). We give here several examples of other processes, starting with a process which exhibits a dynamical phase transition and to which the general results apply directly (see Fig. 6). Then we present other cases which raise

interesting questions which go slightly beyond our present analysis.

A. A dynamical phase transition

Let us consider the system involving two species A and B and the empty state 0:

$$A + A \to A, \quad B + B \to B, \quad A + B \to 0. \quad (59)$$
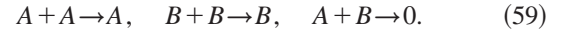
The solutions of Eq. (21) for the fixed points are the empty state $E = (p_A^* = 0, p_B^* = 0, p_0^* = 1)$, the A phase ($p_A^* = 1, p_B^* = 0, p_0^* = 0$), the B phase ($p_A^* = 0, p_B^* = 1, p_0^* = 0$), and the fixed point $C = (p_A^* = \frac{1}{3}, p_B^* = \frac{1}{3}, p_0^* = \frac{1}{3})$.

The A phase and the B phase are attractive fixed points with eigenvalues $\mu_{2,3} = 0$ corresponding to asymptotic exponential decay in $\Gamma = T \ln t$ (i.e., a power law in time) of the other specie. The empty state is a repulsive fixed point with eigenvalues $\mu_{1,2,3} = 1$. The critical point C is attractive for symmetric perturbation $\delta p_A = \delta p_B = -\delta_0/2$ corresponding to eigenvalue $\mu_3 = 0$, but unstable with eigenvalue $\mu_2 = \frac{2}{3}$ for any dissymetric perturbation $\delta p_A \neq \delta p_B$. This corresponds to the exponent $\Phi^-(\frac{2}{3}) = -0.761\,258$ [the other root is $\Phi^+(\frac{2}{3}) = 3.518\,53$]. Since it is globally attractive over the critical manifold, this fixed point controls the dynamical transition from the A phase to B phase. Thus we conclude that if one starts with a system of A and the B in almost equal concentrations, the difference $|p_A(t) - p_B(t)|$ (or equivalently the relative concentrations of A and B) grows with time as

$$|p_A(t) - p_B(t)| \sim (\ln t)^\nu, \quad \nu = 0.761\,258 \quad (60)$$

or, equivalently, the differences of absolute concentrations decay as $|N_A(t) - N_B(t)| \sim (\ln t)^{-2+\nu}$, i.e., more slowly than the decay of both concentrations of A and B, which itself behaves as $(\ln t)^{-2}$. The system eventually reaches a broken symmetry state where either A or B predominates after a time t_{br} which scales as

$$t_{\text{br}} \sim e^{c(t')|p_A(t') - p_B(t')|^{-1/\nu}}, \quad (61)$$

where t' is a (shorter) reference time scale and $c(t')$ a (t'-dependent) constant. Note that the uniform approximation would predict $\nu = 2/3$ significantly smaller than the exact
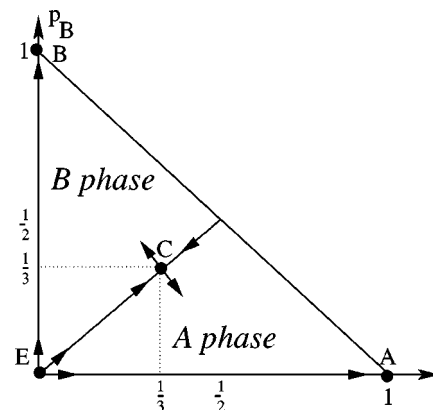

FIG. 6. Dynamical phase diagram of the reaction (59) studied in the text.

result. Finally, the asymptotic final decay of the minority phase is fast, exponential in Γ (as $\mu=0$ at either A ot B fixed points).

Restraining from giving further examples among the large number of possible processes with similarly interesting behavior to which our general results readily apply, we now turn instead to cases where open questions remain.

B. Reaction with a marginal fixed point

Let us now consider the reaction

$$A+A\rightarrow 0, \quad B+B\rightarrow B, \quad A+B\rightarrow 0. \tag{62}$$
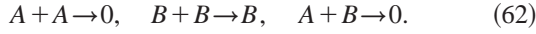
The fixed points are the empty state $E(p_A^*=0,p_B^*=0,p_0^*=1)$ which is unstable with eigenvalues $\mu_{2,3}=1$, the B phase $(p_A^*=0,p_B^*=1,p_0^*=0)$ which is fully attractive with eigenvalues $\mu_{2,3}=0$, and the fixed point $U(p_A^*=\frac{1}{2},p_B^*=0,p_0^*=\frac{1}{2})$ which is attractive with $\mu_3=0$ along the axis $p_B=0$ and marginal with $\mu_2=1/2$ for any perturbation $\delta p_B>0$. Going beyond the linear approximation, we find in the uniform approximation that $\Gamma\partial_\Gamma p_B^\Gamma\simeq 2(p_B^\Gamma)^2$, i.e., a small initial proportion $p_B^{\Gamma_0}$ grows very slowly as

$$p_B^\Gamma\simeq\frac{p_B^{\Gamma_0}}{1-2p_B^{\Gamma_0}\ln\left(\dfrac{\Gamma}{\Gamma_0}\right)} \tag{63}$$

and thus the time scale t_{eq} where the proportion of B becomes finite grows like $\Gamma=T\ln t_{eq}\simeq e^{1/(2p_B^0)}$ for small $p_B^{\Gamma_0}$. In the real dynamics, the exponent $\Phi(\mu=1/2)$ being 0, we also expect a kind of marginal behavior near the fixed point U. A full study of this behavior is an interesting question which goes beyond the present paper.

C. Cyclic reactions and complex eigenvalues

Let us study the reaction

$$A+A\rightarrow A, \quad B+B\rightarrow B, \quad C+C\rightarrow C, \tag{64}$$

$$A+B\rightarrow B, \quad B+C\rightarrow C, \quad C+A\rightarrow A. \tag{65}$$
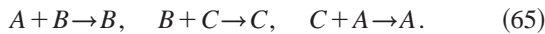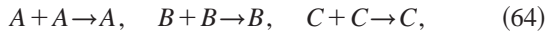
The solutions of Eq. (21) are the three pure phases $p_A=1,p_B=1,p_C=1$ and the mixed state $p_A=p_B=p_C=\frac{1}{3}$. The pure phase $p_A=1$ is stable ($\mu=0$) in the direction $\delta p_C=-\delta p_A>0$, and unstable ($\mu=1$) in the direction $\delta p_B=-\delta p_A>0$. The mixed fixed point $p_A=p_B=p_C=\frac{1}{3}$ has complex eigenvalues $\mu_{2,3}=(1\pm i/\sqrt{3})/2$, leading to purely imaginary naive exponents $\Lambda_{2,3}=\pm i2/\sqrt{3}$. As can be seen in Fig. 5, the exact convergence exponents $\Phi_{2,3}$, solutions of Eq. (52), have a negative real part, and thus the fixed point $p_A=p_B=p_C=\frac{1}{3}$ is also *unstable*. This shows that the asymptotic behavior of the system is more complex than being described by a fixed point of type (21).

In fact, going back to Eq. (32) of the uniform approximation, and eliminating $p_C=1-p_A-p_B$, we obtain that the flow equations for the two variables (p_A,p_B) take the ''divergence-free'' form

$$\Gamma\partial_\Gamma p_A=2\partial_{p_B}f(p_A,p_B), \tag{66}$$

$$\Gamma\partial_\Gamma p_B=-2\partial_{p_A}f(p_A,p_B) \tag{67}$$

with $f(p_A,p_B)=p_Ap_B(1-p_A-p_B)$. As a consequence, all starting points where the three concentrations (p_A,p_B,p_C) are nonzero belong to closed flow lines $p_k^{uniform}(\Gamma)$ of constant value of $f(p_A,p_B)$. Thus in the uniform approximation the asymptotic behavior is always cyclic.

This, however, does not carry to the real dynamics, beyond the uniform approximation, since one can check that these cycles $p_k^{uniform}(\Gamma)e^{-\eta_1-\eta_2}$ are *not* solutions of the RG equation (15). Thus the question of determining the asymptotic behavior of this problem is still open. A more complex cyclic solution, or a new nontrivial fixed point, are among the possibilities.

We close this section by noting that one can also expect from [13,12,14] that reactions with a large enough number of species have chaotic solutions at the level of the uniform approximation. It would be interesting to investigate whether such chaotic solutions could also exist in the RG and in the exact dynamics of these disordered reaction diffusion problems.

D. Reaction with an infinite number of states

We now consider the much studied $A+B\rightarrow$ inert reaction, which, in the absence of disorder, is known to lead to segregation [30] of the two species,

$$A+A\rightarrow A+A, \quad B+B\rightarrow B+B, \quad A+B\rightarrow 0. \tag{68}$$
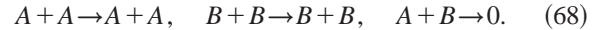
We introduce the notations $A_0=0$, $A_m=mA$, and $A_{-m}=mB$ ($m\geqslant 1$). The possible contents for a valley are now the A_m with $m\in Z$ and thus their number is infinite. The reaction rules become with these notations

$$A_k+A_p\rightarrow A_{k+p}. \tag{69}$$

So for the RG procedure, it is convenient to associate to each valley an auxiliary variable m representing the contents of the valley, and to write the RG equation for the probability distribution $P^\Gamma(z_1,z_2;m)$ where the RG rule for the auxiliary variable m upon fusion of valleys simply reads $m=m_1+m_2$. We can use the result of the Appendix of [64] (for the same RG rule of an auxiliary variable) and obtain the scaling

$$\langle m^2\rangle\sim\Gamma^2. \tag{70}$$

Thus we find that charges of order $\Gamma=T\ln t$ of both signs (i.e., groups of size of order $\Gamma=T\ln t$ of particles of the same specie) will accumulate near the bottom [in a packet of typical size $O(1)$] of each renormalized valley. These packets will be separated by a large distance of order $(T\ln t)^2$. The total number of particles will still decay, as $1/(T\ln t)$. This asymptotic state thus still presents strong features reminiscent of the segregation observed in the pure case [30]. By contrast with the pure model, here several packets of A can also be found in successive neighboring valleys.

V. PERSISTENCE PROPERTIES

We now study persistence properties in the reaction diffusion models defined in Sec. I B. As explained in the Intro-

duction, one is interested in computing probabilities that some type of event has not occured between time 0 and t. The decay with time t of these probabilities usually involves new nontrivial exponents which characterize the nonequilibrium dynamics. Since they integrate over time the behavior of the system, they are usually hard to obtain analytically, even in the pure systems. For reaction diffusion models in a random environment the following types of persistence probabilities can be defined, and will be studied in the following corresponding sections.

(i) The simplest persistence observable is the probability $\Pi(t)$ over runs and environments that a given point $x=0$ has not been crossed by any particle between time 0 and t in a given run. The decay of $\Pi(t)$,

$$\Pi(t) \sim \bar{l}(t)^{-\theta}, \tag{71}$$

where $\bar{l}(t)$ is a characteristic length of the diffusion process, here given from Eq. (10) as $\bar{l}(t) = \frac{1}{2}(T \ln t)^2$, defines the persistence exponent θ. This is the definition used in this paper, even when referring to the pure case, where $\bar{l}(t) \sim \sqrt{t}$, whereas another frequent definition is in terms of the power of t. Since here the diffusion is logarithmic, we choose everywhere in this paper the more general definition (71) both for pure and disordered problems.

(ii) In the presence of quenched disorder one can also study the probability $\Pi_{th}(t)$ over environments that a given point $x=0$ has not been crossed by any of the thermally averaged trajectories $\langle x(t) \rangle$ of the particles. Similarly the decay of $\Pi_{th}(t) \sim \bar{l}(t)^{-\bar{\theta}}$ defines the exponent $\bar{\theta}$. One expects in general that $\bar{\theta} \leq \theta$ and here we find that these two exponents are quite different.

(iii) More generally, one can define the probability that a given pattern present at time 0 has survived up to time t. We study the example of the survival of domains (i.e., intervals between particles), which in the pure case was shown to lead to the definition of two new exponents [46] called δ and ψ: δ characterizes the probability that a domain has survived up to time t without merging with other domains, and ψ characterizes the probability that a domain has survived up to time t with mergings with other domains.

(iv) Finally we study the exponents δ_A and ψ_A characterizing the probability that a particle A has survived up to time t, without any coalescence and with coalescences, respectively.

A. Persistence in a single run

1. No crossing by any particles: Exponent θ

We start by computing the probability $\Pi(t)$ that $x=0$ has not been crossed by *any* particle up to t. We consider a rather general reaction diffusion process with a vacuum state 0 ($k=0$) and occupied states (with particles in them), $k \geq 1$. To solve this problem we can consider separately the two half spaces $x>0$ and $x<0$ and study the problem of a semi-infinite system ($x>0$) with an absorbing boundary at $x=0$ (absorbing for the states $k \geq 1$).

For diffusion in a Sinai landscape in the presence of an absorbing boundary at $x=0$, one defines a new RSRG with slightly new rules: the boundary RSRG, explained in detail
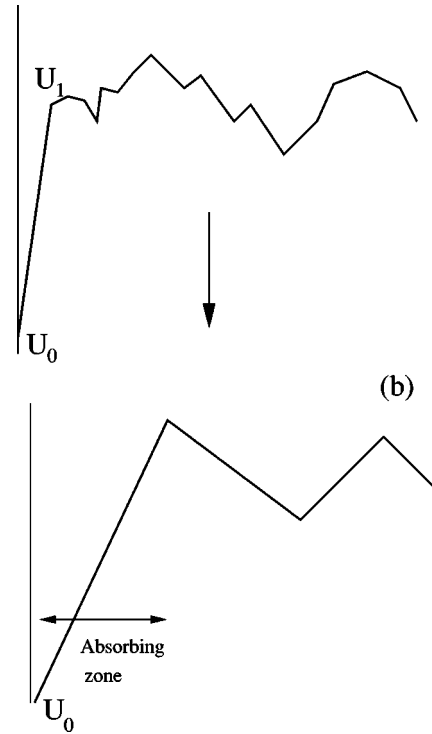

FIG. 7. Illustration of the RG in the presence of an absorbing boundary. (a) The boundary at site $x=0$ can be represented by setting $U_0 = -\infty$. (b) Renormalized landscape, with the absorbing zone (see text).

in Ref. [60]. The first bond is by definition always ascending with an infinite barrier (and thus can never be decimated) and represents an ''absorbing zone'' (see Fig. 7). If the smallest barrier in the system at Γ is the third bond from the boundary or further, the rules are identical to bulk RSRG. If the smallest barrier is the second bond, i.e., the first descending bond, the procedure consists in eliminating the first valley (i.e., the second and third bond) which is merged with the absorbing zone.

Since the reaction rules of the species upon merging valleys are unaffected by the boundary, at a given Γ all renormalized valleys in the bulk are distributed independently with $P_k^\Gamma(\eta_1, \eta_2)$, which satisfies Eq. (15). We now explicitly check that the first renormalized valley also has the same distribution. Indeed the probability $R_k(\eta, \eta')$ that the first renormalized valley has (η, η', k) satisfies the RG equation

$$[\Gamma \partial_\Gamma - (1+\eta)\partial_\eta - (1+\eta')\partial_{\eta'} - 2]R_k^\Gamma(\eta, \eta') \tag{72}$$

$$= P_k^\Gamma(\eta, \eta') \int d\eta_2 \sum_{k'} R_{k'}^\Gamma(0, \eta_2)$$

$$+ W_{k_1,k_2}^k R_{k_1}^\Gamma(\cdot, 0) *_\eta P_{k_2}^\Gamma(\cdot, \eta') \tag{73}$$

$$+ W_{k_1,k_2}^k R_{k_1}^\Gamma(\eta, \cdot) *_{\eta'} P_{k_2}^\Gamma(0, \cdot)$$

$$- R_k^\Gamma(\eta, \eta') \int d\eta_2 \sum_{k'} P_{k'}^\Gamma(0, \eta_2), \tag{74}$$

where the first term corresponds to the decimation of the second bond (which results in the increase of the absorbing

zone) and the old second valley becomes the new first renormalized valley. The third and fourth terms correspond to the decimation of the left bond of the second valley (the loss term must be explicitly written on the left-hand side to keep the distribution R correctly normalized to unity). One can now check that $R_k^\Gamma(\eta,\eta')=P_k^\Gamma(\eta,\eta')$ is a consistent solution.

To compute the persistence exponent, we now define $V_k(\eta,\eta')$ as the probability over all environments that the boundary at $x=0$ has never been crossed by a walker between time 0 and Γ *and* the first renormalized valley has (η,η',k) at Γ. It satisfies the RG equation

$$[\Gamma\partial_\Gamma-(1+\eta)\partial_\eta-(1+\eta')\partial_{\eta'}-2]V_k^\Gamma(\eta,\eta') \qquad (75)$$

$$= P_k^\Gamma(\eta,\eta')\int d\eta_2 V_0^\Gamma(0,\eta_2)$$

$$+ W_{k_1,k_2}^k V_{k_1}^\Gamma(\cdot,0)*_\eta P_{k_2}^\Gamma(\cdot,\eta') \qquad (76)$$

$$+ W_{k_1,k_2}^k V_{k_1}^\Gamma(\eta,\cdot)*_{\eta'} P_{k_2}^\Gamma(0,\cdot)$$

$$- V_k^\Gamma(\eta,\eta')\int d\eta_2 \sum_{k'} P_{k'}^\Gamma(0,\eta_2) \qquad (77)$$

similar to Eq. (72) except for the first term, which carries the restriction that the second bond can be decimated *only if* the first renormalized valley is empty (since, if it contains a particle, this particle gets absorbed by the wall, i.e., crosses the origin). A consistent solution is simply

$$V_k^\Gamma(\eta,\eta')=v_\Gamma P_k^\Gamma(\eta,\eta') \qquad (78)$$

with

$$\Gamma\partial_\Gamma v_\Gamma = -v_\Gamma\int_{\eta_2}\left(\sum_{k'} P_{k'}^\Gamma(0,\eta_2)-P_{k=0}^\Gamma(0,\eta_2)\right). \quad (79)$$

We now use the fact that the system reaches for large Γ an asymptotic state corresponding to an attractive fixed point (20), and this leads to the asymptotic decay

$$v_\Gamma\sim\Gamma^{-(1-p_0^*)}. \qquad (80)$$

Since the probability $\Pi(t)$ that the point $x=0$ has not been crossed by any particle up to time t on the infinite line is the square of the corresponding probability for the semi-infinite problem, we obtain

$$\Pi(t)\sim v_\Gamma^2\sim\bar{l}(t)^{-\theta} \qquad (81)$$

with $\bar{l}(t)=\frac{1}{2}(T\ln t)^2$ and the result for the persistence exponent:

$$\theta=1-p_0^*. \qquad (82)$$

As an example, we show the result for the process (4) where $p_0^*=r/r+1$:

$$\theta_r=\frac{1}{1+r}. \qquad (83)$$

For $r=0$ where the particles A always merge and occupy all valleys, we recover the half-space exponent $\frac{1}{2}\theta(r=0)=\frac{1}{2}$ corresponding to the decay exponent of the probability of no return to the origin for a single Sinai walker obtained in [59,60].

2. Number of particles absorbed by a wall: Generalized persistence

A generalization of the persistence exponent θ can be defined for reaction diffusion models on the semi-infinite line $x>0$ in the presence of an absorbing boundary at $x=0$. There one can compute the probability $Q_\Gamma(n)$ that exactly n particles have been absorbed by the wall up to time t. Generalizing the approach of Eq. (75), we obtain that $Q_\Gamma(n)$ satisfies at large Γ

$$\Gamma\partial_\Gamma Q_\Gamma(n)=(1-p_0^*)[Q_\Gamma(n-1)-Q_\Gamma(n)], \quad n\geqslant 1, \qquad (84)$$

$$\Gamma\partial_\Gamma Q_\Gamma(0)=-(1-p_0^*)Q_\Gamma(0). \qquad (85)$$

The RG equation for the generating function $Q_\Gamma(z)=\Sigma_n z^n Q_\Gamma(n)$,

$$\Gamma\partial_\Gamma Q_\Gamma(z)=-(1-p_0)(1-z)Q(z), \qquad (86)$$

thus leads to the decay $Q_\Gamma(z)\sim\Gamma^{-(1-p_0)(1-z)}$. Introducing the rescaled number of absorbed particles

$$g=\frac{n}{\ln\Gamma} \qquad (87)$$

and using as in [59,60] the saddle point method, we find after a Legendre transform that the probability distribution prob(g) behaves as

$$\text{prob}(g)\sim\Gamma^{-2\omega(g)} \qquad (88)$$

with the generalized persistence exponent

$$2\omega(g)=(1-p_0^*)-g+g\ln\left(\frac{g}{1-p_0^*}\right). \qquad (89)$$

For $g=0$, one recovers the persistence exponent of the half-space $\omega(0)=\theta/2$, where θ is given by Eq. (82). $\omega(g)$ has a zero minimum at $g_a=(1-p_0)$ which is thus the value that g takes with probability 1 as $\Gamma\to\infty$,

$$\frac{n}{\ln(T\ln t)}=(1-p_0^*) \quad \text{with probability 1 as} \quad t\to\infty. \qquad (90)$$

B. Persistence of thermally averaged trajectories

As was discussed in detail in Ref. [60], thermally averaged trajectories of a single Sinai walker follow the effective dynamics which we now use to study their persistence properties. Figure 8 illustrates the difference in the persistence properties between the single run dynamics studied in the preceding section and the effective dynamics of thermally averaged trajectories. Let us consider the case of a valley with a right bond of barrier Γ such that the point $x=0$ lies to
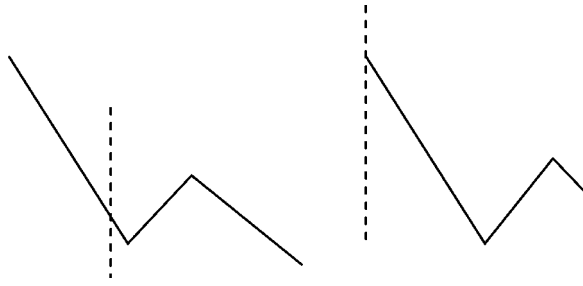
FIG. 8. If the point at $x=0$ (indicated by a dotted line) happens to lie in a renormalized valley as shown on the left figure, it will be crossed many times by a single particle, while it may not be crossed at all by the thermal average $\langle x(t)\rangle$ before it jumps over the barrier on the right. This is not the case in the situation shown on the right figure, where typically no crossing of $x=0$ occurs for a single particle.

the left of a valley bottom and is separated from it by a barrier less than Γ. In this case, $x=0$ will be crossed (several times) in a typical single run, while the thermal average $\langle x(t)\rangle$ will remain at the bottom of the valley until it jumps to the right over the barrier without crossing $x=0$. Thus, as was found in [60] for the return to the origin of a single walker, the exponents θ and $\bar{\theta}$ should generically be different.

We now compute the probability $\Pi_{\text{th}}(t)$ that the point $x=0$ has not been crossed by any particle up to time t within the effective dynamics. Let us define for each valley the auxiliary variables m_1, m_2 equal to the total number of sites in the descending (m_1) and ascending (m_2) bonds, respectively, which have not been crossed by any particle between 0 and t. We define the probabilities $P_k(\eta_1,\eta_2,m_1,m_2)$ that a valley has a specie k, bonds η_1,η_2, and variables m_1,m_2. Consider the decimation represented in Fig. 2. Let us denote the two valleys corresponding to bonds (1,2) and (3,4) containing, respectively, the species k_1 and k_2. Upon decimation of bond 2, the two valleys merge and the specie k_1 jumps to the bottom of the valley (3,4) and thus goes over the bond (2) and (3) to react there with the specie k_2. As a consequence, the auxiliary variable of the new renormalized bond $F_3'=F_1+F_3-\Gamma$ evolves with the rule

$$m_3'=m_1+\delta_{k_1,0}m_2+\delta_{k_1,0}m_3. \tag{91}$$

This is a particular case of the auxiliary variables studied in Appendix A with $a_k=b_k=\delta_{k,0}$ and $d_k=1$.

The final result is that the fraction of sites that have never been crossed by any particle in the effective dynamics decays as $m/\overline{l_\Gamma}\sim(\overline{l_\Gamma})^{-\bar{\theta}}$, where the persistence exponent $\bar{\theta}$ is the solution of the following equation involving the confluent hypergeometric functions $U(a,b,z)$:

$$\bar{\theta}\ U(-p_0^*,2\bar{\theta},1)=U(-p_0^*,2\bar{\theta}+1,1). \tag{92}$$

For the process (4) one has $p_0^*=r/(1+r)$, and the resulting exponent $\bar{\theta}(r)$ is plotted in Fig. 9. Surprisingly we find that it is numerically extremely close for all r (to less than about 1% in relative difference) of *one-half* the result [11] for the pure system, which reads $\frac{1}{2}\theta_{\text{pure}}(r)=-\frac{1}{8}$
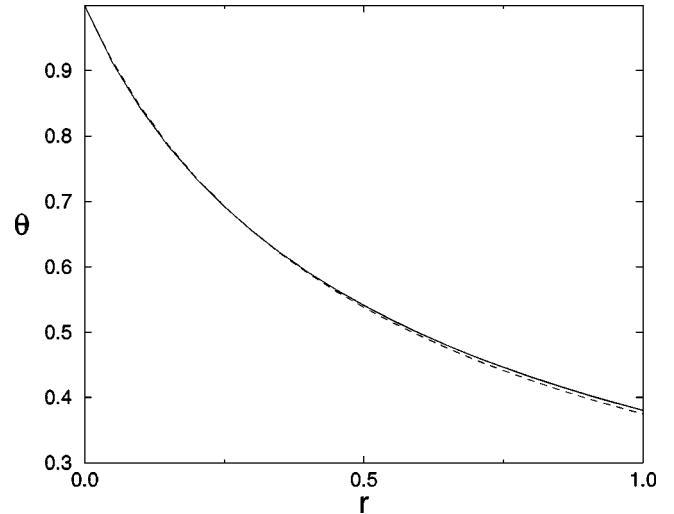

FIG. 9. Plot of $\bar{\theta}(r)$ as a function of r (solid line) and, for comparison, $\frac{1}{2}\theta_{\text{pure}}(r)$ (dashed line).

$+2/\pi^2\{\arccos[(r-1)/\sqrt{2}(r+1)]\}^2$ and is also plotted in Fig. 9. The expansion for small r gives

$$\bar{\theta}(r)=1-2r+o(r), \tag{93}$$

$$\frac{1}{2}\theta_{\text{pure}}(r)=1-\frac{6}{\pi}r+o(r) \tag{94}$$

and thus they are definitively different. In the case $r=1$ where particles always annihilate, we obtain

$$\bar{\theta}(r=1)=0.380\,678\ldots \tag{95}$$

which may be compared with $\frac{1}{2}\theta_{\text{pure}}(r=1)=3/8=0.375$. The difference remains very small for all r, as shown in Fig. 10.

We have also generalized the calculation presented in this section to compute the *number of visits* of thermally averaged trajectories of particles at a given point. It leads again to
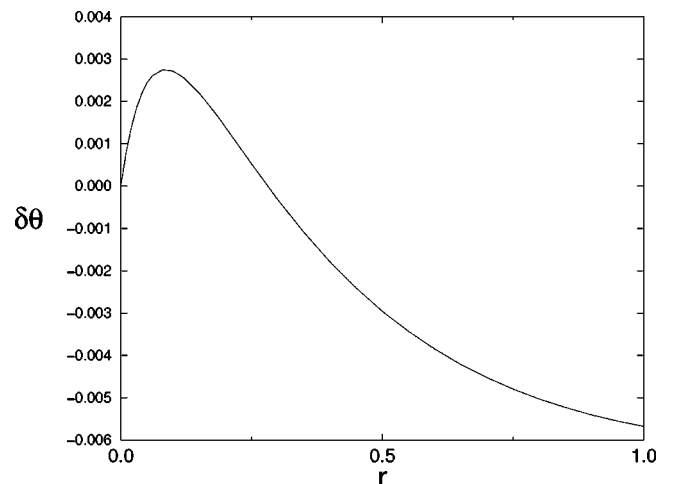

FIG. 10. Plot of $\delta\theta(r)=\frac{1}{2}\theta_{\text{pure}}(r)-\bar{\theta}(r)$: the difference remains very small for all r. It vanishes at $r=0$ and $r=0.280\,701\ldots$.
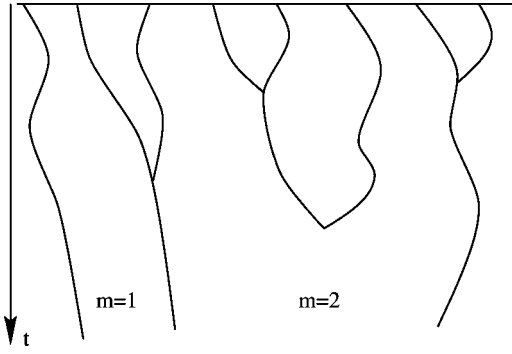
FIG. 11. Diffusion and merging of domains. To each domain present at time t (bottom of the figure) is associated the number m of ancestor domains in the initial state (defined at the top slice $t = 0$). Note that some initial domains die without producing any descendant domain at time t.

a multifractal spectrum of exponents. The calculation and the results are presented in Appendix A.

C. Statistics of merging domains

Here we define domains as intervals between particles. For the reaction (4), on which we now concentrate, when a domain dies (the two particles A meet) the two contiguous domains can either merge if the particles annihilate (with probability r) or remain separate if the particles coalesce (with probability $1-r$). To characterize the statistics of the coarsening of domains in the pure case [i.e., Potts domains with $q = 1+(1/r)$], Krapivsky and Ben-Naim have introduced [46] the following definition. They define $Q_m(t)$ as the number of domains at time t which have for ancestors $m \geqslant 1$ initial domains. This is illustrated in Fig. 11.

The total number $N(t)$ of domains remaining at time t (equal to the total number of A at time t) is simply given by the sum $N(t) = \Sigma_{m=1}^{+\infty} Q_m(t)$ and decays as $\sim p_A^*/\bar{l}(t)$, where $\bar{l}(t) \sim (T \ln t)^2$ is the characteristic length at time t, given in Eq. (10). The fraction of initial domains which have a descendant that is still alive at t is given by $S(t) = \Sigma_m m Q_m(t) = \langle m \rangle N(t)$. The decay of these quantities defines two new independent persistence exponents δ and ψ:

$$Q_1(t) \sim \bar{l}(t)^{-\delta}, \qquad (96)$$

$$S(t) \sim \bar{l}(t)^{-\psi}, \qquad (97)$$

and with these exponents it is expected that $Q_m(t)$ takes the scaling form

$$Q_m(t) = \frac{1}{\bar{l}(t)^{2-\psi}} \mathcal{Q}\left(\frac{m}{\bar{l}(t)^{1-\psi}} \right). \qquad (98)$$

The scaling function is expected to behave for small z as $\mathcal{Q}(z) \sim z^\sigma$, where the exponent σ is related to (δ, ψ) by the relation $\delta = 2 - \psi + (1-\psi)\sigma$. Note that the inequalities $Q_1(t) \leqslant \Sigma_m Q_m(t) \leqslant \Sigma_m m Q_m(t)$ imply that $\psi \leqslant 1 \leqslant \delta$. Note that here we have again defined the exponents with respect to the characteristic length $\bar{l}(t)$ at time t. Thus in the pure case our definition differs from the one of [46] by a factor of 2.

Below, we obtain the exponents $\delta(r)$ and $\psi(r)$ exactly for the process (4).

1. Exponent $\delta(r)$ for the process (4)

For a domain to survive up to time t while keeping its variable $m = 1$, the two domain walls must avoid meeting each other up to time t, but they can meet other exterior domain walls, provided that upon meeting they coalesce and do not annihilate.

Since the two domains walls must not meet, given the properties of the effective dynamics in the RG, the decay of $Q_1(t)$ is governed by the events such that at some Γ_0 the two domains belong to two neighboring renormalized valleys. At all later times they will still belong to two neighboring renormalized valleys and no decimation of the two renormalized bonds separating the two domains can occur. As a consequence, to compute the exponent δ, we can consider separately the two corresponding half-spaces.

For a given half-space, we introduce the probability $R^\Gamma(\eta, \eta')$ that *the first bond has never been decimated* and *the valley is* (η, η') and *there is always one walker in the first valley*. The RG equation for this quantity reads

$$[\Gamma \partial_\Gamma - (1+\eta)\partial_\eta - (1+\eta')\partial_{\eta'} - 2] R^\Gamma(\eta, \eta') \qquad (99)$$

$$= R^\Gamma(\eta, \cdot) *_{\eta'} [P_0^\Gamma(0, \cdot) + (1-r)P_A^\Gamma(0, \cdot)] \qquad (100)$$

$$+ R^\Gamma(\cdot, 0) *_\eta [P_0^\Gamma(\cdot, \eta') + (1-r)P_A^\Gamma(\cdot, \eta')] \qquad (101)$$

$$- R^\Gamma(\eta, \eta') \int_0^\infty d\eta_2 \sum_{k'} P_{k'}^\Gamma(0, \eta_2), \qquad (102)$$

where the $-$ term arises because the R^Γ, unlike the P_k^Γ, is not normalized to 1, and one must count the loss associated with the left bond of the second valley. Integrating over (η, η') one finds that $R^\Gamma = \int d\eta \, d\eta' R^\Gamma(\eta, \eta')$ evolves with

$$\Gamma \frac{dR^\Gamma}{d\Gamma} = - \int d\eta' R^\Gamma(0, \eta') - r p_A^\Gamma \int d\eta \, R^\Gamma(\eta, 0)$$

$$- r R^\Gamma \int_0^\infty d\eta \, P_A^\Gamma(0, \eta) \qquad (103)$$

corresponding to the three forbidden cases: decimation of the first bond, decimation of the second or third bond when both valleys are full, and annihilation occur.

The exponent δ will be given by the decay of the half-space probability $R(\eta, \eta') \sim \Gamma^{-\delta}$, since the probability associated with the two sides will decay as the square of the probility for one side, i.e., as $\Gamma^{-2\delta} \sim \bar{l}_\Gamma^{-\delta}$. Setting $R(\eta, \eta') = \Gamma^{-\delta} e^{-\eta-\eta'} \rho(\eta, \eta')$, and using $p_0^* + (1-r)p_A^* = 1/(1+r)$, one finds

$$0 = [(1+\eta)\partial_\eta + (1+\eta')\partial_{\eta'} + (\delta - 1 - \eta - \eta')] \rho(\eta, \eta') \qquad (104)$$

$$+ \frac{1}{1+r} \left(\int_0^\eta d\eta_1 \rho(\eta_1, 0) + \int_0^{\eta'} d\eta_2 \rho(\eta, \eta_2) \right). \qquad (105)$$
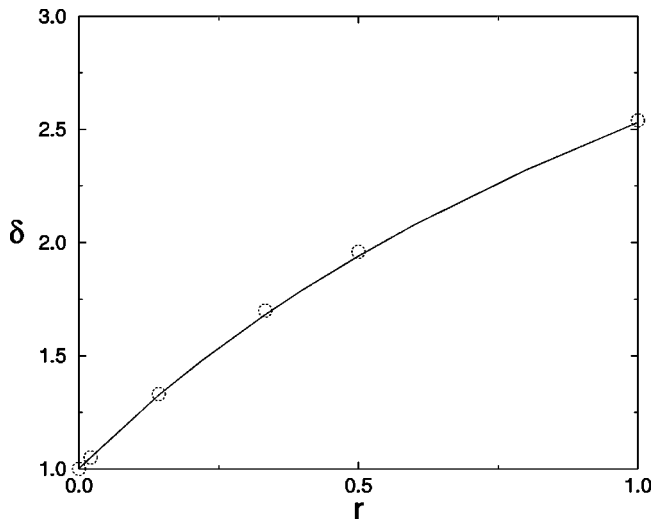
FIG. 12. Plot of the exponent $\delta(r)$ for the process (4) in the Sinai landscape, determined by Eq. (108) (solid line), and comparison with the numerical results of Krapivsky and Ben Naim (Ref. [46]) for the pure case (circles).

There is a solution of the form $\rho(\eta,\eta')=\widetilde{\rho}(\eta+\eta')$, where $\widetilde{\rho}(\eta)$ satisfies

$$0=[(2+\eta)\partial_\eta+(\delta-1-\eta)]\widetilde{\rho}(\eta)+\frac{1}{1+r}\int_0^\eta d\eta'\,\widetilde{\rho}(\eta). \tag{106}$$

After derivation with respect to η, one finds a standard hypergeometric differential equation which allows only for a solution not growing exponentially at $\eta\to\infty$, the confluent hypergeometric function $U(r/r+1,2+\delta,2+\eta)$. The boundary condition at $\eta=0$ then determines the exponent $\delta(r)$ as the solution of the implicit equation

$$2U'\left(\frac{r}{r+1},2+\delta(r),2\right)+[\delta(r)-1]U\left(\frac{r}{r+1},2+\delta(r),2\right)=0. \tag{107}$$

Using the functional relation $zU'(A,B,z)+(B-1-z)U(A,B,z)=-U(A-1,B-1,z)$, the exponent $\delta(r)$ is finally the solution of the equation

$$U\left(-\frac{1}{1+r},1+\delta(r),2\right)=0. \tag{108}$$

The solution of this equation is plotted in Fig. 12.

In the case $r=0$, we find $\delta(r=0)=1$ as expected. Indeed, in that case where particles always coalesce, domains cannot merge, and thus $m=1$ is the only possible value: $Q_m(t)=\frac{1}{l}\,\delta_{m,1}$ and thus $\delta=1=\psi$ as in the pure case. For the case $r=1$, where particles always annihilate, we find

$$\delta(r=1)=2.530\,83\ldots \tag{109}$$

which is remarkably close to the numerical result obtained in [46] for the Ising pure case: $\delta_{\text{pure}}(r=1)=2.54(4)$. This puzzling feature also holds for other values of r, as shown in Fig. 12, with less than about 1% in relative difference.

2. Exponent ψ(r) for the process (4)

To compute ψ we need to obtain the scaling behavior of the average number of ancestors of the domain $\langle m\rangle\sim\Gamma^{2(1-\psi)}$. However, this is a priori difficult, as the variable m is associated to a domain which can extend over many renormalized bonds and is thus "nonlocal." However, we can circumvent this difficulty by decomposing m upon the several renormalized bonds which make up a domain, in order to have a local rule under RG for an auxiliary variable b associated to bonds. Thus we write each variable m for a domain made out of q bonds, as the sum $m=b_1+b_2+\cdots+b_q$, of new auxiliary variables, each associated to a bond. Since q does not grow with Γ, the scaling of $\langle m\rangle$ and $\langle b\rangle$ with Γ is identical. We define RG rules for the local b variables as follows. We consider two neighboring valleys as in Fig. 2 with bonds (1,2) containing specie k_1 and (3,4) containing specie k_2, respectively. One must think of the variable b as counting the number of ancestors associated to a renormalized bond and thus upon decimation of bond (2) the variables b, b' associated to the new bonds of barriers $F_1+F_3-\Gamma$ and F_4 become

$$b=b_1+b_2+b_3 \quad\text{and}\quad b'=b_4 \quad\text{if}\quad k_1=\emptyset, \tag{110}$$

$$b=b_1 \quad\text{and}\quad b'=b_2+b_3+b_4$$
$$\text{if}\quad k_1=A \quad\text{and}\quad k_2=\emptyset, \tag{111}$$

$$b=b_1 \quad\text{and}\quad b'=b_4 \quad\text{if}\quad k_1=A \quad\text{and}\quad k_2=A. \tag{112}$$

The first case where the decimated valley is empty is obvious. In the second case, where a particle A jumps from valley (1,2) to the empty valley (3,4), the ancestors of the domain to the right of A previously associated to the bonds (2), (3), and (4) must now all be associated to the bond (4). In the third case, where the two A meet, the ancestors of (2,3) disappear from the problem in all cases (i.e., annihilation or coalescence of the A particles).

Introducing the rescaled variables $\beta=b/\Gamma^\Phi$, where $\Phi=2(1-\psi)$, the fixed point RG equation for the valley distribution $P_k(\eta,\eta',\beta,\beta')$ reads

$$0=[(1+\eta)\partial_\eta+(1+\eta')\partial_{\eta'}+2$$
$$+\phi(\beta\partial_\beta+\beta'\partial_{\beta'}+2)]P_k(\eta,\eta',\beta,\beta') \tag{113}$$

$$+W_{k_1,k_2}^k\int_{\beta_i}P_{k_1}(\cdot,0,\beta_1,\beta_2)*_\eta P_{k_2}(\cdot,\eta',\beta_3,\beta_4) \tag{114}$$

$$\times\delta\{\beta-[\beta_1+(\beta_2+\beta_3)\delta_{k_1,\emptyset}]\}$$

$$\times\delta\{\beta'-[\beta_4+(\beta_2+\beta_3)\delta_{k_1,A}\delta_{k_2,\emptyset}]\} \tag{115}$$

$$+W_{k_1,k_2}^k\int_{\beta_i}P_{k_1}(\eta,\cdot,\beta_1,\beta_2)*_{\eta'}P_{k_2}(0,\cdot,\beta_3,\beta_4) \tag{116}$$

$$\times\delta\{\beta-[\beta_1+(\beta_2+\beta_3)\delta_{k_1,\varnothing}\delta_{k_2,A}]\}$$

$$\times\delta\{\beta'-[\beta_4+(\beta_2+\beta_3)\delta_{k_2,\emptyset}]\}. \tag{117}$$

We introduce the two first moments ($k=0$ and $k=A$)

$$g_k(\eta,\eta') = \frac{1}{P^*(\eta,\eta')} \int d\beta d\beta' \beta P_k(\eta,\eta',\beta,\beta'), \quad (118)$$

where $P^*(\eta,\eta') = e^{-\eta-\eta'}$.

Using the symmetry $P_k(\eta,\eta',\beta,\beta') = P_k(\eta',\eta,\beta',\beta)$, we find that they satisfy the closed system

$$0 = [(1+\eta)\partial_\eta + (1+\eta')\partial_{\eta'} - \eta - \eta' - \Phi]g_0(\eta,\eta') \quad (119)$$

$$+ p_0^* \int_0^\eta [g_0(\cdot,\eta') + g_0(\cdot,0) + g_0(0,\cdot) + g_A(\cdot,0)]$$

$$+ p_0^* \int_0^{\eta'} [g_0(\eta,\cdot) + g_A(\eta,\cdot)], \quad (120)$$

$$0 = [(1+\eta)\partial_\eta + (1+\eta')\partial_{\eta'} - \eta - \eta' - \Phi]g_A(\eta,\eta') \quad (121)$$

$$+ p_A^* \int_0^\eta [g_A(\cdot,0) + g_0(\cdot,0) + g_0(0,\cdot)] + p_0^* \int_0^\eta g_A(\cdot,\eta') \quad (122)$$

$$+ p_A^* \int_0^{\eta'} [g_A(\eta,\cdot) + g_0(\eta,\cdot) + g_0(\cdot,\eta)]$$

$$+ p_0^* \int_0^{\eta'} g_A(0,\cdot). \quad (123)$$

The exponent Φ is determined by the condition that the solutions $g_0(\eta,\eta')$ and $g_A(\eta,\eta')$ of this system should be well behaved at infinity (i.e., should not be exponentially growing).

We found that setting

$$g_A(\eta,\eta') = S_A(z = \eta + \eta'), \quad (124)$$

$$g_0(\eta,\eta') + g_0(\eta',\eta) = S_0(z = \eta + \eta'), \quad (125)$$

allows us to obtain the following closed system for the two functions $S_0(z)$ and $S_A(z)$:

$$0 = (2+z)S_0'(z) - (z+\Phi)S_0(z) + 2p_0^* \int_0^z [S_0(\cdot) + S_A(z)], \quad (126)$$

$$0 = (2+z)S_A'(z) - (z+\Phi)S_A(z) + \int_0^z [S_A(\cdot) + p_A^* S_0(z)], \quad (127)$$

i.e., independent of the antisymmetric part of $g_0(\eta,\eta')$ which we will not need. To decouple this system, we introduce two linear combinations $S_\pm(z) = c_A S_A(z) + c_0 S_0(z)$ that satisfy closed equations,

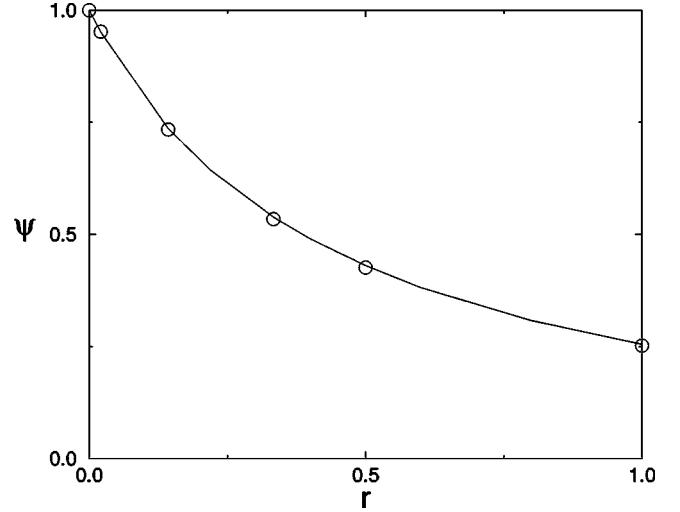$$0 = (2+z)S_\pm'(z) - (z+\Phi)S_\pm(z) + \nu_\pm(r) \int_0^z S_\pm(\cdot), \quad (128)$$

FIG. 13. Plot of the exponent $\psi(r)$ for the process (4) in the Sinai landscape, determined by Eq. (132) (solid line), and comparison with the numerical results of Krapivsky and Ben Naim (Ref. [46]) for the pure case (circles).

where the eigenvalues, using $p_0^* = r/(1+r) = 1 - p_A^*$, are

$$\nu_\pm(r) = \frac{1}{2} + \frac{r}{1+r} \pm \frac{\sqrt{1+6r+r^2}}{2(r+1)}. \quad (129)$$

The only solutions of Eq. (128) that are not exponentially growing at infinity are again given in terms of the degenerate hypergeometric function,

$$S_\pm(z) \propto U(1 - \nu_\pm, 3 - \Phi, 2 + z). \quad (130)$$

The boundary conditions $2S_\pm'(0) = \Phi S_\pm(0)$ finally give

$$U(-\nu_\pm(r), 2\psi_\pm(r), 2) = 0. \quad (131)$$

Since $\psi_+(r) < \psi_-(r)$, the growth of $\langle m \rangle \propto \Gamma^{2(1-\psi)}$ will be governed by $\psi_+(r)$, and thus the final result is that the exponent $\psi(r)$ is determined by the equation

$$U\left(-\frac{1}{2} - \frac{r}{1+r} - \frac{\sqrt{1+6r+r^2}}{2(r+1)}, 2\psi(r), 2\right) = 0. \quad (132)$$

In particular, we have the following expansion around $r = 0$:

$$\psi(r) = 1 - \frac{5}{2}r + o(r). \quad (133)$$

For the case $r = 1$ where particles always annihilate, we find

$$\psi(r=1) = 0.254\,821\ldots \quad (134)$$

which again is remarkably close to the numerical result obtained in [46] for the Ising pure case: $\psi_{\text{pure}}(r=1) = 0.252(2)$, a property which holds again for all r, and again to within less than about 1% in relative difference, as illustrated in Fig. 13.

In the end we note that one can generalize the bound
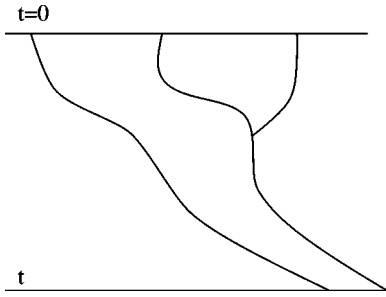
FIG. 14. Configuration where a surviving domain contains no persistent site, which accounts for the strict inequality $\psi(r) < \bar{\theta}(r)$ found here for $r > 0$.

$$\psi_{\text{pure}} \leqslant \theta_{\text{pure}} \qquad (135)$$

discussed in [46], to the disordered case, as

$$\psi(r) \leqslant \bar{\theta}(r), \qquad (136)$$

i.e., that the exponent $\psi(r)$ is always bounded by the persistence exponent $\bar{\theta}(r)$ of thermal averaged trajectories found in Eq. (92). This comes from the observation that a point that has never been crossed by any particle up to time t for the effective dynamics has to belong to a domain that has a descendant still living at time t. Here the reverse inequality is clearly not true (for $p_0^* \neq 0$) since a surviving domain may not contain any persistent site, as it can shift from its initial position, as shown in Fig. 14. In particular, we have found [Eq. (93)]:

$$\bar{\theta}(r) = 1 - 2r + o(r). \qquad (137)$$

Thus $\psi(r)$ and $\bar{\theta}(r)$ differ already at first order in r. This is different from the case of the random field Ising model, studied in [59,61], where it is found that $\psi = \bar{\theta} = (3 - \sqrt{5})/4$, as the situation depicted in Fig. 14 does not occur.

D. Statistics of coalescing particles

We now come to the study of persistence properties associated to a particle. Following the general framework presented in the preceding section for the study of domain merging statistics, we now introduce the number $D_n(t)$ of particles A at time t which have n particles A for ancestors in the initial condition. This is illustrated in Fig. 15. This will lead us to introduce two exponents, δ_A and ψ_A. δ_A has been defined and computed numerically in the pure case in Ref. [77]. We will compute δ_A and ψ_A here in the disordered model.
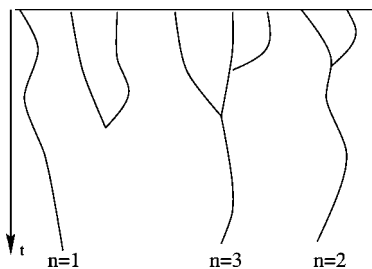

FIG. 15. Number of ancestors of surviving particle.

The total number $N(t)$ of particles at time t is simply given by the sum $N(t) = \Sigma_n D_n(t) \sim (\bar{l}(t))^{-1}$. The fraction of initial particles which have a descendant still alive at t is given by $S_A(t) = \Sigma_n n D_n(t) = \langle n \rangle N(t)$. Again, the decays of $D_1(t)$, i.e., of the number of particles which have encountered no other particles, and of $S_A(t)$ define two new independent exponents,

$$D_1(t) \sim \bar{l}(t)^{-\delta_A}, \qquad (138)$$

$$S_A(t) \sim \bar{l}(t)^{-\psi_A}. \qquad (139)$$

Together with these exponents, it is expected that $D_n(t)$ takes the scaling form

$$D_n(t) = \frac{1}{\bar{l}(t)^{2 - \psi_A}} \mathcal{D}\left(\frac{n}{\bar{l}(t)^{1 - \psi_A}}\right), \qquad (140)$$

where the scaling function behaves for small z as $\mathcal{D}(z) \sim z^{\sigma_A}$ for small z where the exponent σ_A is related to (δ_A, ψ_A) by the relation $\delta_A = 2 - \psi_A + (1 - \psi_A)\sigma_A$.

We will compute these exponents via the RSRG by two methods. The first one is direct, while the second one, presented at the end, will rely on results previously established in Sec. III.

In the first method, we introduce an auxiliary variable n for each valley containing a particle A that counts the number of ancestors of this particle. We then introduce the probability $P_A^\Gamma(\eta, \eta', n)$ that a valley at scale Γ has (η, η') and contains a particle A having n ancestors in the initial condition. It satisfies the RG equation

$$[\Gamma \partial_\Gamma - (1 + \eta)\partial_\eta - (1 + \eta')\partial_{\eta'} - 2] P_A^\Gamma(\eta, \eta', n) \qquad (141)$$

$$= P_A^\Gamma(\eta, \cdot, n) *_{\eta'} P_0^\Gamma(0, \cdot) + P_A^\Gamma(\cdot, 0, n) *_\eta P_0^\Gamma(\cdot, \eta') \qquad (142)$$

$$+ P_0^\Gamma(\eta, \cdot) *_{\eta'} P_A^\Gamma(0, \cdot, n) + P_0^\Gamma(\cdot, 0) *_\eta P_A^\Gamma(\cdot, \eta', n) \qquad (143)$$

$$+ (1 - r)[P_A^\Gamma(\eta, \cdot, \cdot) *_{\eta', n} P_A^\Gamma(0, \cdot, \cdot)$$

$$+ P_A^\Gamma(\cdot, 0, \cdot) *_{\eta, n} P_A^\Gamma(\cdot, \eta', \cdot)], \qquad (144)$$

where $P_0^\Gamma(\eta, \eta')$ is the probability that a valley at scale Γ has (η, η') and contains no particle, i.e., it satisfies Eq. (15). At this stage, the variable n is an integer $n = 1, 2, 3, \ldots$, and the convolution on n is a discrete convolution.

At large Γ, we know the fixed point $P_0^*(\eta, \eta') = p_0^* e^{-\eta - \eta'}$ and $\Sigma_n P_A^*(\eta, \eta', n) = p_A^* e^{-\eta - \eta'}$, where $p_0^* = r/r + 1 = 1 - p_A^*$. Thus setting $P_A^\Gamma(\eta, \eta', n) = p_A^* e^{-\eta - \eta'} \Delta^\Gamma(\eta + \eta', n)$, we find that the function $\Delta^\Gamma(z, n)$ satisfies

$$[\Gamma \partial_\Gamma - (2 + z)\partial_z + z] \Delta^\Gamma(z, n)$$

$$= 2 p_0^* \int_0^z dz' \Delta^\Gamma(z', n) + (1 - r) p_A^* \Delta^\Gamma(\cdot, \cdot) *_{z, n} \Delta^\Gamma(\cdot, \cdot)$$

$$(145)$$

and we now will compute successively $\delta_A(r)$, $\psi_A(r)$ for all r and the scaling function for $r=0$.

1. Exponent $\delta_A(r)$ for the process (4)

To compute the exponent δ_A giving the decay of the number of particles A that have only one ancestor in the initial condition, we need to solve the previous equation for the particular value $n=1$. $\Delta^{\Gamma}(z, n=1)$ decouples from the other values of n, and satisfies the linear equation

$$[\Gamma \partial_{\Gamma} - (2+z)\partial_z + z]\Delta^{\Gamma}(z,1) = 2p_0^* \int_0^z dz' \Delta^{\Gamma}(z',1). \quad (146)$$

Since

$$D_{n=1}(t) = N(t)\int_{\eta,\eta'} P_A^{\Gamma}(\eta,\eta',1) \sim (1/\Gamma^2)\int dz z e^{-z}\Delta^{\Gamma}(z,1),$$

we set $\Delta^{\Gamma}(z,1) = \Gamma^{2-2\delta_A}\Delta(z)$. The function $\Delta(z)$ is then the solution of the differential equation

$$(2+z)\Delta''(z) + (2\delta_A - 1 - z)\Delta'(z) - (1 - 2p_0^*)\Delta(z) = 0 \quad (147)$$

together with the boundary condition at $z=0$,

$$2\Delta'(0) + (2\delta_A - 2)\Delta(0) = 0. \quad (148)$$

We thus find $\Delta(z) \propto U(1 - 2p_0^*, 1 + 2\delta_A, 2+z)$, and the exponent δ is determined by the implicit equation

$$2U'(1 - 2p_0^*, 1 + 2\delta_A, 2) + (2\delta_A - 2)U(1 - 2p_0^*, 1 + 2\delta_A, 2)$$
$$= 0. \quad (149)$$

Using the functional relation $zU'(A,B,z) + (B - 1 - z)U(A,B,z) = -U(A-1,B-1,z)$, and $p_0^* = r/r+1$, the exponent $\delta_A(r)$ is finally the solution of the equation

$$U\left(-\frac{2r}{r+1}, 2\delta_A(r), 2\right) = 0. \quad (150)$$

For the particular case $r=1$ where particles always annihilate upon meeting, we have $\delta_A(r=1) = 1$ as it should since in this case the particles can have only one ancestor $D_n(t) = \delta_{n,1}N_A(t)$. In the limit $r \to 0$, where particles always coalesce upon meeting, we have $\delta_A(r=0) \to +\infty$: indeed in this case at large Γ, all valleys contain a particle A ($p_A^* = 1$), and the probability to have $n=1$ decays exponentially with Γ, since it requires that four consecutive bonds (the two bonds of the valley and the two neighbors) are not decimated. One can compare with the pure case ($\delta_A = 2\theta 1$ in notations of [77]) where $\delta_A(1) = 1$ but $\delta_A(r=0) = 3$.

2. Exponent $\psi_A(r)$ for the process (4)

To compute the exponent ψ_A, we introduce the rescaled variable $\nu = n/\Gamma^{2(1-\psi_A)}$. The fixed point solution $\Delta(z,\nu) = P_A^*(z,\nu)/p_A^* e^{-z}$ of the rescaled variables has to satisfy

$$[(2+z)\partial_z - z + 2(1-\psi_A)(\nu\partial_{\nu} + 1)]\Delta(z,\nu) \quad (151)$$

$$+2p_0^* \int_0^z dz' \Delta(z',\nu) + (1-r)p_A^* \Delta(\cdot,\cdot)*_{z,\nu}\Delta(\cdot,\cdot) = 0. \quad (152)$$

In particular, using $p_0^* = r/(r+1) = rp_A^*$, we find that its first moment $C(z) = \int_0^{\infty} d\nu\, \nu\Delta(z,\nu)$ satisfies the differential equation

$$(2+z)C''(z) + (2\psi_A - 1 - z)C'(z) + (1 - 2p_0^*)C(z) = 0 \quad (153)$$

with the boundary condition at $z=0$,

$$2C'(0) + 2(\psi_A - 1)C'(0) = 0. \quad (154)$$

So finally $C(z) \propto U(-1 + 2p_0^*, 1 + 2\psi_A, 2+z)$, where the exponent ψ_A is the solution of the implicit equation

$$2U'(-1 + 2p_0^*, 1 + 2\psi_A, 2)$$
$$+ 2(\psi_A - 1)U(-1 + 2p_0^*, 1 + 2\psi_A, 2) = 0. \quad (155)$$

Using again the functional relation $zU'(A,B,z) + (B - 1 - z)U(A,B,z) = -U(A-1,B-1,z)$, and $p_0^* = r/r+1$, the exponent $\psi_A(r)$ is finally the smaller solution of the equation

$$U\left(-\frac{2}{1+r}, 2\psi_A(r), 2\right) = 0. \quad (156)$$

For the particular case $r=1$ where particles always annihilate upon meeting, we have $\psi_A(r=1) = 1 = \delta(r=1)$ as it should, since in this case the particles can have only one ancestor. In the case $r=0$, where particles always coalesce upon meeting, we have $\psi_A(r=0) = 0$: indeed the probability for an initial particle to have a descendant living at Γ is 1, and thus $S_A(t)$ is constant and not decaying.

3. Scaling function

The distribution $\mathcal{D}(\nu)$ of the rescaled variable $\nu = n/\Gamma^{(2-2\psi_A)}$ can in principle be obtained in terms of the solution $\Delta(z,\nu)$ of Eq. (151) as

$$\mathcal{D}(\nu) = \int_0^{\infty} d\eta_1 \int_0^{\infty} d\eta_2 \frac{P_A^*(\eta_1,\eta_2,\nu)}{p_A^*} = \int_0^{\infty} dz\, z e^{-z}\Delta(z,\nu). \quad (157)$$

In Laplace with respect to ν, we have that $\hat{\Delta}_r(z,q) = \int_0^{\infty} d\nu\, e^{-q\nu}\Delta_r(z,\nu)$ satisfies

$$\{(2+z)\partial_z - z - 2[1 - \psi_A(r)]q\partial_q\}\hat{\Delta}_r(z,q) \quad (158)$$

$$+ \frac{2r}{1+r}\int_0^z dz' \hat{\Delta}(z',q) + \frac{1-r}{1+r}\hat{\Delta}_r(\cdot,q)*_z\hat{\Delta}_r(\cdot,q) = 0. \quad (159)$$

In the case $r=0$, where particles always coalesce upon meeting, the number n of ancestors should have the same statistical properties as the length of a valley, and thus using the fixed point solution we should have

TABLE I. Summary of the results obtained in the text for persistence exponents associated to the decay of the probability of each indicated event, in the case of the reaction diffusion process $A+A \to \emptyset$ (prob r)$A+A \to A$ (prob $1-r$).

Event	Exponent	Equation
No crossing of O by any particle	$\theta(r)$	$\theta = 1/(1+r)$
$n = g \ln \Gamma$ particles absorbed at O	$\omega(g)$	$2\omega = (1+r)^{-1} - g + g \ln[(1+r)g]$
No crossing of O by thermal. aver. traj.	$\bar{\theta}(r)$	$\bar{\theta} U\left(-\dfrac{r}{1+r}, 2\bar{\theta}, 1\right) = U\left(-\dfrac{r}{1+r}, 2\bar{\theta}+1, 1\right)$
Domain survival without merging	$\delta(r)$	$U(-1/(1+r), 1+\delta, 2) = 0$
Domain survival with merging	$\psi(r)$	$U\left(-\dfrac{1}{2} - \dfrac{r}{1+r} - \dfrac{\sqrt{1+6r+r^2}}{2(r+1)}, 2\psi, 2\right) = 0$
Particle survival without coalescence	$\delta_A(r)$	$U(-2r/(1+r), 2\delta_A, 2) = 0$
Particle survival with coalescence	$\psi_A(r)$	$U(-2/(1+r), 2\psi_A, 2) = 0$

$$\int_0^\infty d\nu \, e^{-q\nu} \frac{P_A^*(z,\nu)}{p_a^*} = \frac{q}{\sinh^2 \sqrt{q}} e^{-z\sqrt{q} \coth \sqrt{q}}. \quad (160)$$

Indeed we find

$$\hat{\Delta}_{r=0}(z,q) = \frac{q}{\sinh^2 \sqrt{q}} e^{z(1-\sqrt{q}\coth\sqrt{q})} \quad (161)$$

is the solution of Eq. (158) for $(r=0, \psi_A=0)$, and thus in this case the scaling function $\mathcal{D}(\nu)$ reads

$$\mathcal{D}_{r=0}(\nu) = LT_{q \to \nu}^{-1}\left(\frac{1}{\cosh^2 \sqrt{q}}\right)$$

$$= \sum_{j=-\infty}^{+\infty} [2\nu\pi^2(j+1/2)^2 - 1]e^{-\nu\pi^2(1/2+j)^2} \quad (162)$$

$$= \frac{2}{\sqrt{\pi}\nu^{3/2}} \sum_{k=-\infty}^{+\infty} (-1)^{k+1} k^2 e^{-k^2/\nu}. \quad (163)$$

4. Second method to compute $\delta_A(r)$ and $\psi_A(r)$

To compute $D_1(t)$, i.e., the probability that a given particle A has met no other particles up to time t, we can consider this particle A as a tagged particle, say X, and consider it as a new specie in very small concentration. It satifies the following reaction rule:

$$A+X \to 0, \quad \text{prob} = 1 \quad (164)$$
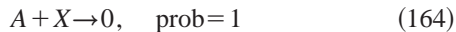
and of course $X+0 \to X$ and the same reactions for the A as before. We need only to work to linear order in p_X and we are back exactly in the case studied in Sec. III of the dynamics near the asymptotic state of a new reaction diffusion (whose fixed point has $p_X^* = 0$). The corresponding eigenvalue of the matrix M introduced in Eq. (22) is $\mu = p_0^* = r/(1+r)$. Here $0 \leqslant \mu \leqslant 1/2$, which corresponds to an attractive fixed point at $p_X = 0$ (since the X disappears) and with $p_X \sim \Gamma^{-\Phi}$, where Φ is solution of Eq. (52) for $\mu = r/(1+r)$. Since $D_1(t) \sim p_X/\Gamma^2 \sim \Gamma^{-2\delta_A}$, we recover Eq. (150).

To compute the exponent $\psi_A(r)$ we need to consider similarly the reaction for the tagged particle X:

$$A+X \to X, \quad \text{prob} = 1-r, \quad (165)$$

$$A+X \to 0, \quad \text{prob} = r, \quad (166)$$
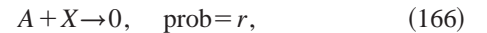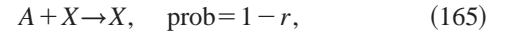
and of course $X+0 \to X$ and the same reactions for the A. In this case $\mu = p_0^* + p_A^*(1-r) = 1/(1+r)$ and $1/2 < \mu < 1$, which corresponds to an *unstable* fixed point at $p_X = 0$. One finds $p_X \sim \Gamma^{-\Phi}$, where Φ is the solution Φ_- of Eq. (52) for $\mu = 1/(1+r)$. Since $S_A(t) \sim p_X/\Gamma^2 \sim \Gamma^{-2\psi_A}$ we recover Eq. (156) which determines $\psi_A(r)$ (see Table I).

VI. DISORDER IN THE REACTION PROBABILITIES

It is interesting to study the stability of our results to an additional quenched disorder in the reaction probabilities given by the matrix W (i.e., spatial inhomogeneities). We continue to consider only the rule that species react immediately when they encounter, but the analysis in fact also covers — in an effective way — the case where reaction rates are finite and with quenched disorder. We sketch in this section a possible way of applying the present RSRG procedure to this case.

Let us consider a model where the reaction probabilities are themselves functions of the position $W_{k_1,k_2}^k(x)$. A simple example is to allow the parameter r to depend on x as $r(x)$ in the process (4). Let us examine what happens at a decimation time scale $\Gamma = T \ln t$. The particle in state k_1 in the decimated valley jumps over the barrier to a valley containing k_2. Since k_2 is typically at equilibrium at the bottom of its valley, the reaction is most likely to take place at the bottom of the valley within a $O(1)$ distance of it (since this is where all the weight of the particule k_2 is concentrated). Thus as time increases, the total number of sites in the system where reactions can typically occurs decays as $1/\Gamma^2$. In each renormalized valley at Γ there is typically a ''finite'' number (i.e., not growing with Γ) of sites x where reactions occur and thus a ''finite'' number of possible values $W(x)$ (a notation for the set of W_{k_1,k_2}^k). For each valley these form a given set fixed in time. There are thus *a priori* two competing effects: the several values taken by W in a valley result in an ''averaging'' effect for the effective W of this valley. On the other

hand, the fact that this set is finite and fixed in time implies nontrivial correlations between two reactions occurring at different times in the same valley.

Here we will restrict ourselves to considering a toy model where we assign a single transition matrix W to each renormalized valley with probability $P(W)$. It would be accurate in the case where in the initial distribution the W's are correlated over distances much larger than the typical thermal width of a packet $\sim O(1)$, but still small compared to Γ^2. This problem can thus be treated by introducing the probability $P_k(\eta_1, \eta_2, W)$ that a valley has rescaled barriers η_1, η_2 and an associated rate W. When two valley merge upon a decimation, the new one simply keeps the W of the lowest one. One notes that the statistical independence is again preserved by RG. The RG equation is simply

$$
\begin{aligned}
\Gamma \partial_\Gamma P_k^\Gamma(\eta_1, \eta_2, W) \\
= [(1+\eta_1)\partial_{\eta_1} + (1+\eta_2)\partial_{\eta_2} + 2] P_k^\Gamma(\eta_1, \eta_2, W) \\
+ W_{k_1, k_2}^k [P_{k_1}^\Gamma(\eta_1, \cdot, W) *_{\eta_2} P_{k_2}^\Gamma(0, \cdot) \\
+ P_{k_1}^\Gamma(\cdot, 0) *_{\eta_1} P_{k_2}^\Gamma(\cdot, \eta_2, W)],
\end{aligned}
\tag{167}
$$

where $\int_W P_k(\eta_1, \eta_2, W) = P_k(\eta_1, \eta_2)$ and summation over repeated indices is implied. We also note that the distribution of W, $P_\Gamma(W) = \Sigma_k \int_{\eta_1, \eta_2} P_k(\eta_1, \eta_2, W)$, is preserved by the RG rule, thus $P^\Gamma(W) = P(W)$. Thus we have a ''marginal'' problem, since in this toy model $P(W)$ does not flow by RG [76].

One can now look for fixed points of this RG equation under the form

$$
P_k(\eta_1, \eta_2, W) = e^{-\eta_1 - \eta_2} P_k(W),
\tag{168}
$$

where the $P_k(W)$ must satisfy

$$
P_k(W) = W_{k_1, k_2}^k P_{k_2}(W) \int dW' P_{k_1}(W').
\tag{169}
$$

In the case of the model (4) with a distribution $P(r)$ of r, one can show that a solution is

$$
P_k(r) = P(r) p_k^*(r),
\tag{170}
$$

where $p_0^*(r) = r/(1+r)$ and $p_A^*(r) = 1/(1+r)$ are the equilibrium occupation probabilities for the problem with a uniform r solution of the equation $p_k^*(W) = W_{k_1, k_2}^k p_{k_2}^*(W) p_{k_1}^*(W)$. Such a simple solution holds in that case because of the form of the matrix M (22) which is simply a projector onto the vector p_k^*. In general, this does not hold and one has to solve the above equation. It is then possible in principle to perform, for an arbitrary $P(W)$, the same study as the one done here, such as stability eigenvalues around the fixed point, etc., which is left for the future.

To summarize, the above result indicates that within the toy model and the effective dynamics, quenched disorder in the transition matrix $W(x)$ will lead to a modification of the large time properties. These properties can be computed using the RG by assigning an effective reaction probability matrix of each valley. They depend in a continuous way on the asymptotic distribution $P(W)$. There is thus an infinite

dimensional manifold of fixed points in the RG sense, and the problem is *marginal*. Like all marginal problems, it is very sensitive to corrections which may make disorder marginally irrelevant or marginally relevant (or remain strictly marginal). The averaging effect may in the end make the disorder marginally irrelevant, but to decide, within the real dynamics [76] and within a model with shorter disorder correlation length, whether disorder is actually marginally irrelevant, and how it flows, requires a more detailed study which goes beyond this work.

VII. CONCLUSION

In this paper we have studied the problem of various species of particles diffusing in the presence of quenched random local bias (Sinai landscape) and reacting upon meeting. We have shown that the real space renormalization group method (RSRG), which has proved to be a powerful tool to study single particle diffusion in the Sinai landscape [59], can be extended in a simple and natural way to study a large class of reaction diffusion models. Since here also the physics is controlled by infinitely broad disorder fixed points, this method, as in the single particle problem, is expected to yield the *exact* large time behavior. Focusing on renormalized valleys as well as on the particles (and species) contained in these valleys, and following the evolution of their distribution by decimation upon an increase of the time scale, allowed us to obtain many new exact results for this problem.

We have obtained a detailed description of the asymptotic states, such as the large time decay of the density of each specie, $n_k(t)$, and the spatial distribution of particles. It confirms that in the $d=1$ Sinai landscape the reaction is subdiffusion limited. The first step was to identify simple fixed points of the valley distribution RG equation, which correspond — for a given reaction process described by a transition matrix — to possible asymptotic dynamical states. Each of these states is characterized by fixed fractions p_k^* for each specie, the physical picture being the following. At time scale $\Gamma = T \ln t$ the system consists of a set of successive renormalized valleys, which can be either empty, with probability $p_\emptyset^*$, or contain a particle of specie k, with probability p_k^*. The separation between particles grows as the characteristic length $\bar{l}(t) \sim \Gamma^2$, and thus $n_k(t) \sim p_k^*/(T \ln t)^2$. The decay of concentration, when compared to the single particle diffusion length, leads us to define universal amplitudes, which we obtained exactly. Also, from the exact statistical independence of the successive valley lengths, the distribution of intervals between particles (domains) was derived (and compared with some pure case results).

To confirm that a given fixed point is indeed an asymptotic state, actually reached by the system at large time, it is necessary to study its linear stability. We have thus obtained analytically the spectrum of stability eigenvalues around any simple fixed point, as a function of the reaction transition matrix, thereby solving the stability problem. The convergence towards these asymptotic states (i.e., the attractive RG fixed points) was studied. The leading convergence towards these asymptotic states was found to be generically as $|p_k(t) - p_k^*| \sim (T \ln t)^{-\Phi}$ with a nontrivial Φ solution of a hypergeometric equation (with, in addition, an amplitude periodic in $\ln t$ in the case of complex eigenvalues). In some

cases, corresponding to $\Phi = +\infty$, the convergence is faster as a power law in time with nonuniversal exponents depending on details of the initial model.

Eigenvalues corresponding to unstable fixed points, which were also determined, are of particular interest for reactions which lead to several distinct dynamical phases (i.e., several possible asymptotic states). The transitions between different dynamical phases being controlled by such unstable RG fixed points, we have thus obtained the corresponding critical exponents. As an example, a process with a nontrivial phase diagram was studied.

We have also studied persistence properties associated to a given asymptotic state. As in pure systems, where it was originally defined, persistence can be studied for various types of patterns (single particles, domains, etc.). Remarkably, for the disordered models at hand we are able to derive a *much larger* set of exact results than exists at present for the corresponding pure systems.

We have first obtained, for a generic process, the decay exponent θ for the probability of no crossing of a given point by single particle trajectories. As noted in [59], in a disordered system, persistence of thermal averages can be quite different from single particle persistence. Thus we have also computed the probability of no crossing of a given point by thermally averaged packets, which yields the decay exponent $\bar{\theta}$. The properly generalized persistence exponents associated to n crossings have been defined, and computed. Next, we have characterized the statistics of domains, which can disappear or merge as time increases. Restricting, for simplicity, to the process $A + A \rightarrow \emptyset$ or A with probabilities $(r, 1-r)$, we have obtained exactly the exponents $\delta(r)$ and $\psi(r)$ characterizing the survival up to time t of a domain without any merging or with mergings, respectively. We have also introduced new exponents which similarly characterize the statistics of the coalescence of particles. We have then computed them, namely $\delta_A(r)$ and $\psi_A(r)$, characterizing the survival up to time t of a particle A without any coalescence or with coalescences, respectively.

We have found these new exponents as solutions of hypergeometric equations. For comparison, the only known analytical result in the pure case is for the exponent $\theta_{\text{pure}}(r)$ for the process (4). A surprising outcome was that several exact exponents of the model with disorder were found to be numerically very close, for all values of r, to some exponents for the pure system, although they are associated to a completely different diffusion length $[l_{\text{pure}} \sim \sqrt{t}$ while $\bar{l}(t) \sim (T \ln t)^2]$. Indeed we found that $\bar{\theta}(r) \approx \frac{1}{2}\theta_{\text{pure}}(r)$ although they are definitely distinct, and furthermore that $\psi(r) \approx \psi_{\text{pure}}(r)$ and $\delta(r) \approx \delta_{\text{pure}}(r)$, where $\psi_{\text{pure}}(r)$, $\delta_{\text{pure}}(r)$ — not known analytically — are extracted from the numerical simulation of [46]. The agreement in relative values is better than about 1% for all r. It may be that this observed numerical coincidence could be traced to the exact statistical independence of valley lengths in the disordered problem, while the so-called ''independent interval approximation'' gives a reasonable approximation in the pure case (but, surprisingly, poorer than the one provided by these new exponents). This, however, is far from an explanation and further investigation may be of interest.

The effect of additional disorder in the reaction rates was also discussed. In a simple case it was found to be marginal, and thus yield nontrivial modifications, continuously varying with the disorder distribution. The question of whether this result is stable with respect to corrections resulting from the real dynamics or from disorder with shorter correlation length remains to be further investigated

Although we have not considered explicitly branching BARW processes, with additional creation of particles, it is clear that for at least some of them the physics should not be qualitatively too different from the one obtained here. Indeed, since in Sinai disorder particles are essentially confined to the bottom of large renormalized wells, as long as the process is such that particles are not created out of the vacuum and that the annihilation reactions are sufficient to maintain the number of particles small when at local equilibrium in a well, the reaction can be treated very similarly via RSRG as for the model studied here. We have thus characterized a broad set of reaction diffusion models with disorder.

Finally, it is worthwhile to mention that we have also identified cases which clearly require a more complicated analysis going beyond the present paper. For instance, we have given an example of a marginal reaction, which requires a nonlinear stability analysis. Also, we have given an example of a cyclic reaction for which all simple RG fixed points are shown to be unstable. The question of the determination of the true asymptotic states of this reaction is thus still open. Another interesting, and maybe related, question is whether reactions with a large enough number of species, which can lead to chaotic attractors in pure cases [12,13], will also lead to chaotic behavior in the presence of disorder.

APPENDIX A: AUXILIARY VARIABLE FOR VALLEYS

In this appendix we study auxiliary variables (m) associated to bonds that evolve upon decimation as follows. Consider the decimation of bond (2) in Fig. 2: the two valleys corresponding to bonds (1,2) and (3,4) and containing, respectively, the species k_1 and k_2 merge, and the specie k_1 jumps to the bottom of valley (3,4) and thus goes over the bond (2) and (3) to react there with the specie k_2. It is thus natural to consider an auxiliary variable m which, upon decimation of the barrier $F_3' = F_1 + F_3 - \Gamma$, evolves with the general rule

$$m_3' = d_{k_1} m_1 + b_{k_1} m_2 + a_{k_1} m_3, \qquad \text{(A1)}$$

where the coefficients (a_k, b_k, d_k) depend on the specie k which diffuses upon the corresponding decimation.

We now write the valley RG equation for $P_k^\Gamma(\eta, \eta', m, m')$:

$$[\Gamma \partial_\Gamma - (1+\eta)\partial_\eta - (1+\eta')\partial_{\eta'} - 2]P_k^\Gamma(\eta, \eta', m, m') \qquad \text{(A2)}$$

$$= W^k_{k_1,k_2} \int_{m_1,m'_1,m_2,m'_2} \tag{A3}$$

$$\times [P^\Gamma_{k_1}(\eta,\cdot,m,m'_1) *_{\eta'} P^\Gamma_{k_2}(0,\cdot,m_2,m'_2)$$

$$\times \delta(m' - a_{k_2}m'_1 - b_{k_2}m_2 - d_{k_2}m'_2) \tag{A4}$$

$$+ P^\Gamma_{k_1}(\cdot,0,m_1,m'_1) *_\eta P^\Gamma_{k_2}(\cdot,\eta',m_2,m')$$

$$\times \delta(m - d_{k_1}m_1 - b_{k_1}m'_1 - a_{k_1}m_2)]. \tag{A5}$$

Integrating this equation over the m variables one recovers of course the specie valley RG equation (15).

We now define the first moment:

$$G^1_k(\eta_1,\eta_2) = \int_{m_1,m_2} m_1 P_k(\eta_1,\eta_2,m_1,m_2), \tag{A6}$$

$$G^2_k(\eta_1,\eta_2) = \int_{m_1,m_2} m_2 P_k(\eta_1,\eta_2,m_1,m_2). \tag{A7}$$

Since we are looking at the symmetric case, we have that $G^2_k(\eta_1,\eta_2) = G^1_k(\eta_2,\eta_1)$. We can thus write the following closed equation for $G^1_k(\eta_1,\eta_2)$:

$$[\Gamma \partial_\Gamma - (1+\eta_1)\partial_{\eta_1} - (1+\eta_2)\partial_{\eta_2} - 2]G^1_k(\eta_1,\eta_2) \tag{A8}$$

$$= W^k_{k_1,k_2}[G^1_{k_1}(\eta_1,\cdot) *_{\eta_2} P_{k_2}(0,\cdot)$$

$$+ a_{k_1} P_{k_1}(\cdot,0) *_{\eta_1} G^1_{k_2}(\cdot,\eta_2) \tag{A9}$$

$$+ b_{k_1} G^1_{k_1}(0,\cdot) *_{\eta_1} P_{k_2}(\cdot,\eta_2)$$

$$+ d_{k_1} G^1_{k_1}(\cdot,0) *_{\eta_1} P_{k_2}(\cdot,\eta_2)]. \tag{A10}$$

In the asymptotic state we use the fixed point solution $P^*_k(\eta_1,\eta_2) = p^*_k e^{-\eta_1-\eta_2}$, and write $G^1_k(\eta_1,\eta_2) = e^{-\eta_1-\eta_2} g_k(\eta_1,\eta_2)$ and obtain the equation for the new function g_k:

$$\Gamma \partial_\Gamma g_k(\eta_1,\eta_2) = [(1+\eta_1)\partial_{\eta_1} - \eta_1$$

$$+ (1+\eta_2)\partial_{\eta_2} - \eta_2]g_k(\eta_1,\eta_2) \tag{A11}$$

$$+ W^k_{k_1,k_2}\left(p^*_{k_2} \int_0^{\eta_2} g_{k_1}(\eta_1,\cdot)\right.$$

$$+ p^*_{k_1} a_{k_1} \int_0^{\eta_1} g_{k_2}(\cdot,\eta_2) \tag{A12}$$

$$+ p^*_{k_2} b_{k_1} \int_0^{\eta_1} g_{k_1}(0,\cdot)$$

$$\left. + p^*_{k_2} d_{k_1} \int_0^{\eta_1} g_{k_1}(\cdot,0)\right). \tag{A13}$$

Since the m variable is associated to bonds, it is natural to look for solutions where the function $g_k(\eta_1,\eta_2)$ is a function of η_1 alone. We thus try solutions of the form

$g^\Gamma_k(\eta_1,\eta_2) = \Gamma^\psi g_k(\eta_1)$, where the exponent ψ characterizes the scaling of the m variable $m \sim \Gamma^\psi$.

For this to work we obtain, in terms of the matrix M defined in Eq. (22), the necessary condition

$$g_k(\eta) = W^k_{k_1 k_2} p^*_{k_2} g_{k_1}(\eta) = M_{k,k_1} g_{k_1}(\eta) \tag{A14}$$

together with the differential equation for $g_k(\eta)$:

$$0 = [(1+\eta)\partial_\eta - \eta - \psi]g_k(\eta)$$

$$+ (M_{k,k_1} d_{k_1} + W^k_{k_1,k_2} p^*_{k_2} a_{k_2}) \int_0^\eta g_{k_1}(\cdot)$$

$$+ M_{k,k_1} b_{k_1} g_{k_1}(0)\eta. \tag{A15}$$

One can then try $g_k(\eta) = p^*_k \psi(\eta)$, which automatically satisfies the necessary condition (A14) above (since p^*_k is by construction an eigenvector of the M matrix of eigenvalue 1), and then the second equation gives the conditions involving two numbers $\lambda_{1,2}$,

$$M_{k,k_1} p^*_{k_1}(d_{k_1} + a_{k_1}) = \lambda_1 p^*_k, \tag{A16}$$

$$M_{k,k_1} p^*_{k_1} b_{k_1} = \lambda_2 p^*_k, \tag{A17}$$

together with the differential equation for $g(\eta)$:

$$0 = [(1+\eta)\partial_\eta - \eta - \psi]g(\eta) + \lambda_1 \int_0^\eta \psi(\cdot) + \lambda_2 \psi(0)\eta. \tag{A18}$$

We now give two applications of this general analysis.

1. Persistence exponent $\bar\theta$

We now study the case $a_k = b_k = \delta_{k,0}$ and $d_k = 1$ corresponding to the auxiliary variable (A1) needed to compute the persistence exponent $\bar\theta$. Conditions (A16) become

$$p^*_k + M_{k,0} p^*_0 = \lambda_1 p^*_k, \tag{A19}$$

$$M_{k,0} p^*_0 = \lambda_2 p^*_k. \tag{A20}$$

Since the rates involving the empty state (0) are given by definition by $W^k_{i0} = \delta_{k,i}$, we have $M_{k,0} = W^k_{0,i} p^*_i = \delta_{k,i} p^*_i = p^*_k$. The conditions above are thus satisfied with $\lambda_1 = 1 + p^*_0$ and $\lambda_2 = p^*_0$ and thus the problem reduces to studying Eq. (A18) for $g(\eta)$:

$$0 = [(1+\eta)\partial_\eta - \eta - \psi]g(\eta) + (1+p^*_0)$$

$$\times \int_0^{\eta_1} g(\cdot) + p^*_0 g(0)\eta_1. \tag{A21}$$

Differentiating with respect to η one gets

$$0 = (1+\eta)\partial^2_\eta g(\eta) + (1 - \phi - \eta)\partial_\eta g(\eta) + p^*_0[g(\eta) + g(0)] \tag{A22}$$

with the boundary condition $g'(0) = \psi g(0)$. The solution of this confluent hypergeometric equation that is a well behaved solution at infinity (i.e., not growing exponentially) reads

$$g(\eta)=g(0)\left(2\frac{U(-p_0^*,2-\phi,1+\eta)}{U(-p_0^*,2-\phi,1)}-1\right). \quad (A23)$$

The boundary condition at $\eta=0$ then leads to the following equation for the exponent ψ governing the scaling of the m variable $m\sim\Gamma^\psi$, as a function of p_0^*:

$$U'(-p_0^*,2-\psi,1)=\frac{\psi}{2}U(-p_0^*,2-\psi,1). \quad (A24)$$

Using functional relations of the confluent hypergeometric functions U, we finally obtain that the fraction of sites that have never been crossed by any particle in the effective dynamics decays as $m/\overline{l_\Gamma}\sim\Gamma^{\psi-2}\sim(\overline{l_\Gamma})^{-\overline{\theta}}$, where the persistence exponent $\overline{\theta}=(2-\psi)/2$ is a solution of the equation

$$\overline{\theta}\ U(-p_0^*,2\overline{\theta},1)=U(-p_0^*,2\overline{\theta}+1,1). \quad (A25)$$

2. Number of thermal packets seen by a given point

We introduce the bond variable $m(n)$ which is the number of sites on the bond which have been crossed exactly n times by a particle (any nonempty state) in the effective dynamics (i.e., by a thermally averaged trajectory). It satisfies upon decimation of bond (2) with the same conventions as above:

$$m_3'(n)=m_1(n)+m_2(n-1)+m_3(n-1) \quad \text{if } k_1\neq0, \quad (A26)$$

$$m_3'(n)=m_1(n)+m_2(n)+m_3(n) \quad \text{if } k_1=0. \quad (A27)$$

Introducing the generating function $m(z)=\sum_{n=0}^{n=+\infty}m(n)z^n$, the rule becomes

$$m_3'(z)=d_{k_1}(z)m_1(z)+b_{k_1}(z)m_2(z)+a_{k_1}(z)m_3(z) \quad (A28)$$

which, for fixed z, is the same rule as above with now $a_k(z)=b_k(z)=\delta_{k,0}+z(1-\delta_{k,0})$ and $d_k=1$. Conditions (A16) become

$$(1+z)p_k^*+(1-z)M_{k,0}p_0^*=\lambda_1 p_k^*, \quad (A29)$$

$$zp_k^*+(1-z)M_{k,0}p_0^*=\lambda_2 p_k^* \quad (A30)$$

and thus using again $W_{i0}^k=\delta_{k,i}$ these conditions are satisfied with $\lambda_1(z)=1+z+(1-z)p_0^*$ and $\lambda_2=z+(1-z)p_0^*$, i.e., we only need to perform the substitution $p_0^*\rightarrow z+p_0^2(1-z)$ in the previous solution to obtain the equation for the exponent $\overline{\theta}(z)$ governing the scaling of the ratio $m(z)/\overline{l_\Gamma}\sim(\overline{l_\Gamma})^{-\overline{\theta}(z)}$:

$$\overline{\theta}(z)U(-z-p_0(1-z),2\overline{\theta}(z),1)$$
$$=U(-z-p_0(1-z),1+2\overline{\theta}(z),1). \quad (A31)$$

The probability that a given point has been visited by n thermally averaged trajectories up to time t is thus obtained in the rescaled variable $g=n/\ln\Gamma$ as

$$\text{prob}(g)\sim(\overline{l_\Gamma})^{-\overline{\theta}(g)}. \quad (A32)$$

It decays with the exponent $\overline{\theta}(g)$ obtained through the Legendre transform

$$2\overline{\theta}(g)=2\overline{\theta}(z^*(g))+g\ln(z^*(g)), \quad (A33)$$

where $z^*(g)$ is the solution of $2[\overline{\theta}(z)/dz]+g/z=0$.

One can compute simply the value g_a that g takes with probability 1 as $\Gamma\rightarrow\infty$. It is given by $\overline{\theta}(g_a)=0=\overline{\theta}(g)/dg|_{g=g_a}$. This gives $g_a=-2[\overline{\theta}(z)/dz]|_{z=1}$, and thus differentiating Eq. (A31) with respect to z and taking $z=1$ we finally get

$$g_a=(1-p_0^*)\frac{U_1(-1,1,1)}{U(-1,0,1)/2-U_2(-1,1,1)}=\frac{4}{3}(1-p_0^*), \quad (A34)$$

where we have used the notations $U_1(a,b,z)\equiv\partial_a U(a,b,z)$ and $U_2(a,b,z)\equiv\partial_b U(a,b,z)$.

APPENDIX B: THE PARTICULAR CASE OF "ASSOCIATIVE PROCESSES"

It turns out to be useful to introduce the notion of "associative processes:" these are processes such that the outcome of a sequence of reactions does not depend on the order in which it was performed, i.e., such that the rates W satisfy

$$W_{p_1\alpha}^k W_{p_2p_3}^\alpha=W_{p_2\beta}^k W_{p_1p_3}^\beta \quad (B1)$$

for all k,p_1,p_2,p_3 (contraction over α and β is implied). This means that the probability of $(p_2p_3)p_1=k$ is identical to the probability of $(p_1p_3)p_2=k$ (ab denotes the result of the reaction of a and b). For example, the process defined in Eq. (4) is associative.

An important property of associative processes is that their matrix M (22) satisfies

$$M^2=M \quad (B2)$$

and thus the eigenvalues μ_α have only two possible values: 0 or 1.

For the RG, these processes have also the following interesting property: the subspace of valley distributions of the form

$$P_k^\Gamma(\eta_1,\eta_2)=W_{r_1,r_2}^k P_{r_1}^\Gamma(\eta_1)P_{r_2}^\Gamma(\eta_2) \quad (B3)$$

is conserved by the RG (15), provided that the bond distribution $P_k^\Gamma(\eta)$ satisfies the bond RG equation

$$\Gamma\partial_\Gamma P_k^\Gamma(\eta)=[(1+\eta)\partial_\eta+1]P_k^\Gamma(\eta)$$
$$+W_{k',k_3}^k W_{k_1,k_2}^{k'}P_{k_2}^\Gamma(0)P_{k_1}^\Gamma(\cdot)*_\eta P_{k_3}^\Gamma(\cdot).$$
$$(B4)$$

The bond RG equation (B4) can in fact be interpreted to characterize the following modified reaction diffusion process, which we call "the bond-reaction diffusion process:"

one associates to the bottom of each bond (i.e., the point of lowest energy) a specie in one of the possible ''states'' and defines probability distributions $P_k(z)$ for the bonds. We consider two consecutive valleys made with the bonds $(1,2)$ and $(3,4)$. Initially the bonds $(1,2,3,4)$, respectively, contain the species k_1,k_2,k_3,k_4. Upon decimation of bond (2), the bond diffusion process is defined as follows in three steps. (i) First the two species k_1,k_2 on bonds $(1,2)$ react to give another state k' with the rates $W^{k'}_{k_1,k_2}$. (ii) The new specie k' diffuses towards the bottom of the bond 3. (iii) The species (k',k_3) react at the bottom of bond 3 to give a new species k'_3 with the rates $W^{k'_3}_{k',k_3}$. For comparison, it is useful to recall

the corresponding real dynamics with valleys: initially, the valley $(1,2)$ contains some species k', the valley $(3,4)$ some species k''. Upon decimation of bond (2), the species k' diffuses towards the bottom of the valley $(3,4)$ and reacts therewith k'' to give k with probability $W^k_{k',k''}$. Thus, in the end, the physical content (the specie) of the renormalized valley for the bond-diffusion process is k with probability $W^k_{k'_3,k_4}W^{k'_3}_{k',k_3}$, whereas in the original valley process, the final result is k with probability $W^k_{k',k''}W^{k''}_{k_3,k_4}$. The two descriptions are thus equivalent in that sense only if the rates satisfy the associativity condition (B1).

---

[1] *Nonequilibrium Statistical mechanics in One Dimension*, edited by V. Privman (Cambridge University Press, Cambridge, 1997).

[2] M.V. Smoluchovsky, Z. Phys. Chem., Stoechiom. Verwandtschaftsl. **92**, 129 (1917).

[3] A.A. Ovchinnikov and Y.B. Zeldovich, Chem. Phys. **28**, 215 (1978).

[4] For review, see V. Kuzovkov and E. Kotomin, Rep. Prog. Phys. **51**, 1479 (1998).

[5] For review, see J. L. Cardy, e-print cond-mat/9607163; in Proceedings of Mathematical Beauty of Physics, edited by J.B. Zuber [Adv. Ser. in Math. Phys. **24**, 113 (1997)].

[6] For a review see A.J. Bray, Adv. Phys. **43**, 357 (1994).

[7] A.J. Bray, B. Derrida, and C. Godreche, Europhys. Lett. **27**, 175 (1994); A.D. Rutenberg and A.J. Bray, Phys. Rev. E **50**, 1900 (1994); A.J. Bray and B. Derrida, *ibid.* **51**, R1633 (1995); B. Derrida, C. Godreche, and I. Yekutieli, Europhys. Lett. **12**, 385 (1990); Phys. Rev. A **44**, 6241 (1991).

[8] P.L. Krapivsky, E. Ben Naim, and S. Redner, Phys. Rev. E **50**, 2474 (1994).

[9] S.N. Majumdar and C. Sire, Phys. Rev. Lett. **77**, 1420 (1996).

[10] K. Oerding, S. J. Cornell, and A. J. Bray, e-print cond-mat/9702203; Phys. Rev. E **56**, R25 (1997).

[11] B. Derrida, V. Hakim, and V. Pasquier, Phys. Rev. Lett. **75**, 751 (1995).

[12] See, e.g., M.V. Velikanov and R. Kapral, e-print chao-dyn/9804014.

[13] P. Peeters and G. Nicolis, Physica A **188**, 426 (1992).

[14] J. Coste, J. Peyraud, and P. Coullet, J. Stat. Phys. **21**, 33 (1979); SIAM J. Appl. Math. **36**, 516 (1979).

[15] P. Coullet, Thèse de Doctorat, Nice, 1980 (unpublished).

[16] L. Peliti, J. Phys. (Paris) **46**, 1469 (1985).

[17] J. L. Cardy and U. C. Tauber, e-print cond-mat/9704160; J. Stat. Phys. (to be published).

[18] P. Grassberger and K. Sundermeyer, Phys. Lett. **77B**, 220 (1978).

[19] J. Cardy, J. Phys. A **16**, L709 (1983).

[20] H.K. Janssen, Z. Phys. B **58**, 311 (1985).

[21] K. Mussawisade, J.E. Santos, and G.M. Schutz, e-print cond-mat/9801104.

[22] F. Van Wijland, K. Oerding, and H. J. Hilhorst, e-print cond-mat/9706197; Physica A **251**, 179 (1998); J. Phys. A (to be published).

[23] F. Van Wijland, These de Doctorat, Universite Paris–Sud, 1998 (unpublished).

[24] S.P. Obhukov, Pisma Zh. Éksp. Teor. Fiz. **45**, 139 (1987) [JETP Lett. **45**, 172 (1987)].

[25] H.K. Janssen, Phys. Rev. E **55**, 6253 (1997).

[26] A.G. Moreira and R. Dickman, Phys. Rev. E **54**, R3090 (1996).

[27] B.P. Lee, J. Phys. A **27**, 2633 (1994).

[28] L. Peliti, J. Phys. A **19**, L365 (1986).

[29] K. Kang and S. Redner, Phys. Rev. A **30**, 2833 (1984); Phys. Rev. Lett. **52**, 955 (1984); Phys. Rev. A **32**, 435 (1985).

[30] Z.Y. Cheng, Phys. Rev. Lett. **59**, 1726 (1987).

[31] For a short review, see A. Cadilhe, M. L. Glasser, and V. Privman, e-print cond-mat/9606224; Int. J. Mod. Phys. B. (to be published).

[32] B.P. Lee and J. Cardy, J. Stat. Phys. **80**, 971 (1995).

[33] M. Bramson and J.L. Lebowitz, Phys. Rev. Lett. **62**, 297 (1991).

[34] J.M. Park and M.W. Deem, Phys. Rev. E **58**, 3223 (1998).

[35] M.W. Deem and J.M. Park, Phys. Rev. E **57**, 3618 (1998); **57**, 2681 (1998).

[36] K. Oerding, J. Phys. A **29**, 7051 (1996).

[37] D.S. Fisher, D. Friedan, Z. Qiu, S.J. Shenker, and S.H. Shenker, Phys. Rev. A **31**, 3841 (1985).

[38] J.P. Bouchaud, A. Comtet, A. Georges, and P. Le Doussal, J. Phys. (Paris) **48**, 1445 (1987).

[39] M.J.E. Richardson and J. Cardy, e-print cond-mat/9901217.

[40] See, however, [68] and discussion below.

[41] The question of the extrapolation to $d=1$ models, via a $d=2-\epsilon$ expansion, is subtle, as can be seen already for the single particle diffusion. Within the context of single particle diffusion with short range Gaussian disorder; there are in $d=2$ *three* distinct RG fixed points [37]: (i) purely divergence-free (hydrodynamic) flows, (ii) purely potential disorder; (iii) mixed disorder. Since only pure potential disorder can exist in $d=1$, the most natural approach to describe the Sinai model in $d=1$ would be to extrapolate while remaining within the class of potential disorder models (ii). This is delicate, however, as discussed in [38], as models (ii) have a vanishing beta function in $d=2$: they are described by a line of fixed points in $d=2$ while presumably by a strong disorder (nonperturbative) fixed point for any $d<2$. Another possiblity would be to extrapolateng down to $d=1$ starting from the mixed disorder fixed

point (iii) (as was done, e.g., in Ref. [39]) as it is natural to assume that as $d \rightarrow 1$ the fixed points (ii) and (iii) merge. However, since (ii) and (iii) have a completely different physics and symmetries in $d=2$, one may expect that, although workable, this expansion would be rather poor, as can be seen already as $z = 2 + 2\epsilon^2$ while $z = +\infty$ in $d=1$. The increase of reaction rate observed at (iii) in $d=2$ in Ref. [39] (while we prove the opposite effect for Sinai disorder in $d=1$) is evidence of the different physics between (iii) and (ii). Finally, concerning the random barrier or trap models (with broad distributions of waiting times) in $d=1$ [40], they are truly a different universality class and we do not see any reason why they could be reached by extrapolating Gaussian disorder in $d=2$.

[42] The mapping extends to random bonds, each walker (domain wall) seeing a potential equal to the local bond strength J. Diffusion of the Potts domains in a Sinai landscape then would correspond to Glauber dynamics in a Potts model with *correlated* bond randomness (of correlator growing proportional to the distance). In addition to not being very physical, such randomness would also lead—at large enough scale—to sign changes in bonds, invalidating the assumption $T \ll J$ necessary to treat the Glauber dynamics by the present method. The process (4), however, remains interesting and fully well defined, as a reaction diffusion problem in the presence of disorder, and results can be compared to the nontrivial ones obtained for the pure case. This is thus the point of view that we choose in this paper.

[43] A.A. Lushnikov, Phys. Lett. A **120**, 135 (1987).

[44] B. Derrida, V. Hakim, V. Pasquier, J. Stat. Phys. **85**, 763 (1996).

[45] B. Derrida and R. Zeitak, Phys. Rev. E **54**, 2513 (1996).

[46] P.L. Krapivsky and E. Ben Naim, Phys. Rev. E **56**, 3788 (1997).

[47] L. Frachebourg, P.L. Krapivsky, and S. Redner, Phys. Rev. E **55**, 6684 (1997).

[48] S. Cueille and C. Sire, e-print cond-mat/9707287; J. Phys. A **30**, L791 (1997); Eur. Phys. J. B **7**, 111 (1999).

[49] I. Dornic and C. Godreche, e-print cond-mat/9712178; J. Phys. A **31**, 5413 (1998).

[50] M. Howard and C. Godreche, e-print cond-mat/9711148; J. Phys. A **31**, L209 (1998).

[51] J. Krug *et al.*, e-print cond-mat/9704238; Phys. Rev. E **56**, 2702 (1997).

[52] Y.G. Sinai, Probab. Appl. **27**, 247 (1982).

[53] H. Kesten, M. Koslov, and F. Spitzer, Compositio Mathematica **30**, 145 (1975).

[54] H. Kesten, Physica A **138**, 299 (1986).

[55] B. Derrida, J. Stat. Phys. **31**, 433 (1983).

[56] J.P. Bouchaud, A. Comtet, A. Georges, P. Le Doussal, Europhys. Lett. **3**, 653 (1987); Ann. Phys. (N.Y.) **201**, 285 (1990).

[57] A. Comtet, J. Desbois, and C. Monthus, Ann. Phys. (N.Y.) **239**, 312 (1995); C. Monthus *et al.*, Phys. Rev. E **54**, 231 (1996).

[58] L. Laloux and P. Le Doussal, e-print cond-mat/9705249; Phys. Rev. E **57**, 6296 (1998), and references therein.

[59] D.S. Fisher, P. Le Doussal, and C. Monthus, e-print cond-mat/9710270; Phys. Rev. Lett. **80**, 3539 (1998).

[60] P. Le Doussal, C. Monthus, and D. S. Fisher, Phys. Rev. E **59**, 4795 (1999).

[61] D.S. Fisher, P. Le Doussal, and C. Monthus (unpublished).

[62] C. Dasgupta and S.K. Ma, Phys. Rev. B **22**, 1305 (1980).

[63] D.S. Fisher, Phys. Rev. B **50**, 3799 (1994).

[64] D.S. Fisher, Phys. Rev. B **51**, 6411 (1995).

[65] C. Monthus, O. Golinelli, and T. Jolicoeur, Phys. Rev. Lett. **79**, 3254 (1997).

[66] See, e.g., F. C. Alcaraz, M. Droz, M. Henkel, and V. Rittenberg, e-print hep-th/9302112; Ann. Phys. (N.Y.) **230**, 250 (1994).

[67] S. N. Majumdar and A. J. Bray, e-print cond-mat/9805380; Phys. Rev. Lett. **81**, 2626 (1998).

[68] G. M. Schutz and K. Mussawisade, e-print cond-mat/9801103; Phys. Rev. E **57**, 2563 (1998).

[69] We will denote everywhere the dependence of all quantities in the variable Γ by a superscript, which should not be confused for a power.

[70] Note that the definition of the symbol $\bar{l}_\Gamma$ is different from the one used in [60] where it denoted the averaged length of a valley.

[71] t_0 depends only on the details of single particle dynamics on short scales.

[72] It is independent of k [71].

[73] Keeping in mind the cautionary remarks in [41], we can still attempt to compare with the $d = 2 - \epsilon$ expansion formula (14) from [39], which reads $\mathcal{A} = 0.106103(1/\epsilon) + 0.0263539 + O(\epsilon)$ and leads to $\mathcal{A} \sim 0.13$ by setting $\epsilon = 1$.

[74] Restoring the microscopic time unit t_0, one notes that the coefficient c of the $O(1/\Gamma)$ correction in n_Γ can be set to 0 by a redefinition of the microscopic time scale t_0 [71]. This redefinition does not affect the formula for the $p_k(t)$ as it corresponds to the landscape eigenvector with $\Phi = +1$.

[75] The case of a nondiagonalizable block of degenerate eigenvalues also deserves a separate study, not performed here. It is likely to lead to additional logarithmic corrections ($\ln \Gamma$ and powers of it) to the large time behavior.

[76] Within this toy model there will be corrections due to rare events which split the thermal packet between distants wells. For instance, events (a) in Fig. 7 of [60] tend to average the disorder in the W. However, they occur with probability at most of order $O(1/\Gamma)$ and should not affect the leading behavior. A detailed study of these corrections goes beyond this paper.

[77] S. N. Majundar and S. J. Cornell, Phys. Rev. E **57**, 3757 (1998).